 USGS-OFR-84-172

UNITED STATES DEPARTMENT OF THE INTERIOR

GEOLOGICAL SURVEY

REPORT ON TELEVIEWER LOG AND STRESS MEASUREMENTS IN CORE HOLE USW G-2, NEVADA TEST SITE OCTOBER-NOVEMBER, 1982

By

J. M. Stock, J. H. Healy, and S. H. Hickman

Open-File Report 84-172

Prepared in cooperation with the
Nevada Operations Office, U. S. Department of Energy
(Interagency Agreement DE-AI08-78ET44802)

CONTENTS

ILLUSTRATIONS

TABLES

UNITED STATES
DEPARTMENT OF THE INTERIOR
GEOLOGICAL SURVEY

REPORT ON TELEVIEWER LOG AND STRESS MEASUREMENTS IN CORE HOLE USW G-2, NEVADA TEST SITE OCTOBER-NOVEMBER, 1982

By

J. M. Stock, J. H. Healy, and S. H. Hickman

....

ABSTRACT

Hydraulic fracturing stress measurements and a borehole televiewer log were obtained in hole USW G-2 at Yucca Mountain, Nevada, to depths of 1200 m. Results indicate that at the depths tested, the minimum and maximum horizontal stresses are less than the vertical stress, corresponding to a normal faulting stress regime. Drilling-induced hydrofractures seen in the televiewer log imply a least horizontal principal stress direction of N 60° W to N 65° W. For reasonable values of the coefficient of friction, the magnitude of the least horizontal stress is close to the value at which slip would occur on preexisting faults of optimal orientation (strike N 25° E to N 30° E and dipping 60° to 67°).

The prominent drilling-induced fractures seen in the televiewer log are believed to have been caused by excess downhole pressures applied during drilling the hole. Many throughgoing fractures are also seen in the televiewer log; most of these are high angle, stringking N 10° E to N 40° E. These fractures show a general decrease in angle of dip with depth. Stress-induced wellbore breakouts are seen at depths below 1050 m. The average N 60° W azimuth of these breakouts agrees very closely with the N 60° W to N 65° W direction of least horizontal principal stress inferred from the drilling-induced hydrofracs.

INTRODUCTION

This report describes the operations and preliminary results of televiewer logging and stress measurements done between October 10 and November 5, 1982, in core hole USW G-2 on Yucca Mountain, at the western boundary of the Nevada Test Site. USW G-2 is one of a series of holes in which these measurements are being performed, to collect information on the state of stress in the vicinity of Yucca Mountain. The results of these stress studies, and of a variety of other geological, geophysical, and hydrologic investigations in the Nevada Nuclear Waste Storage Investigations (NNWSI) Project, will be used to evaluate the area as a potential repository for radioactive waste.

Two separate techniques, borehole televiewer logging and hydraulic fracturing (hydrofracturing), were used to gain information about the current state of stress at USW G-2. First, an ultrasonic borehole televiewer was used to map fractures and other irregular features of the borehole wall and to identify smooth, unfractured sections of the borehole suitable for stress measurements. Directions of the principal stresses were determined from the orientations of hydrofractures induced during drilling. Second, magnitudes of the principal stresses were determined from the pressure-volume time curves of hydrofracture tests, in which a short section of the borehole is isolated with rubber packers and the rock is fractured by fluid pressure applied through tubing from the surface. A comparison of the USW G-2 measurements with measurements made in other holes at Yucca Mountain (USW G-1 and UE25p-1) is also presented.

ACKNOWLEDGEMENTS

We thank Joseph Svitek, Dennis Styles, Jackie Hennagan, Larry Mastin, and Gretchen Zwart for assistance in the field operations.

LOCATION AND GEOLOGIC SETTING

USW G-2 is a core hole drilled to a depth of 1829 m (6000 ft) at Nevada state coordinates 778,825 N, 560,503 E (36°53'22" N latitude, 116°27'35" W longitude), on the east flank of Yucca Mountain (Figure 1). Ground level elevation at the site is 1554 m (5098 ft). The hole penetrates volcanic units of welded to nonwelded tuffs with minor bedded tuff, lava flows, and breccia zones. The stratigraphic section extends from the Tiva Canyon Member of the Paintbrush Tuff, at the surface, to the Lithic Ridge Tuff and older tuffs at the bottom of the hole (Figure 2). Study of the core shows strong variation in the degree of welding and alteration, and significant fracturing in all units except the nonwelded and zeolitized tuffaceous beds of Calico Hills (Maldonado and Koether, 1983).

The same stratigraphic units from hole UE25a-1 (4.6 km SE of USW G-2) show a wide variation in porosity in the interval from the Tiva Canyon Member to the Crater Flat Tuff, with porosity as low as 8% in parts of the Topopah Springs Member and as high as 35% in the tuffaceous beds of Calico Hills (Anderson, 1981). Core specific gravity measurements and borehole gravimetry tied to gamma-gamma well log measurements in holes USW H-1 and USW G-1 (both about 3 km SSE of USW G-2) give average density values for these volcanic units ranging from 1.90 g/cm^3 for the tuffaceous beds of Calico Hills to approximately 2.40 g/cm^3 for the older tuffs (Snyder and Carr, 1982). The wide range of porosities, densities, and alteration present in the rocks in USW G-2 is reflected in the televiewer observations and in the hydrofracture behavior of the rock units in the tested intervals (discussed below).

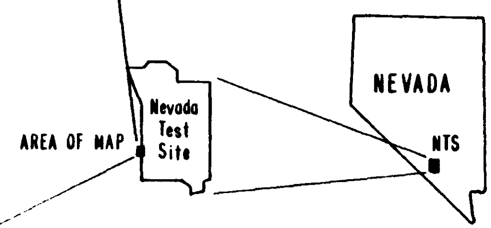

Figure 1. Map showing location of hole USW G-2 and other holes discussed in text. White is outcrop of volcanics, and stippled pattern represents alluvium.

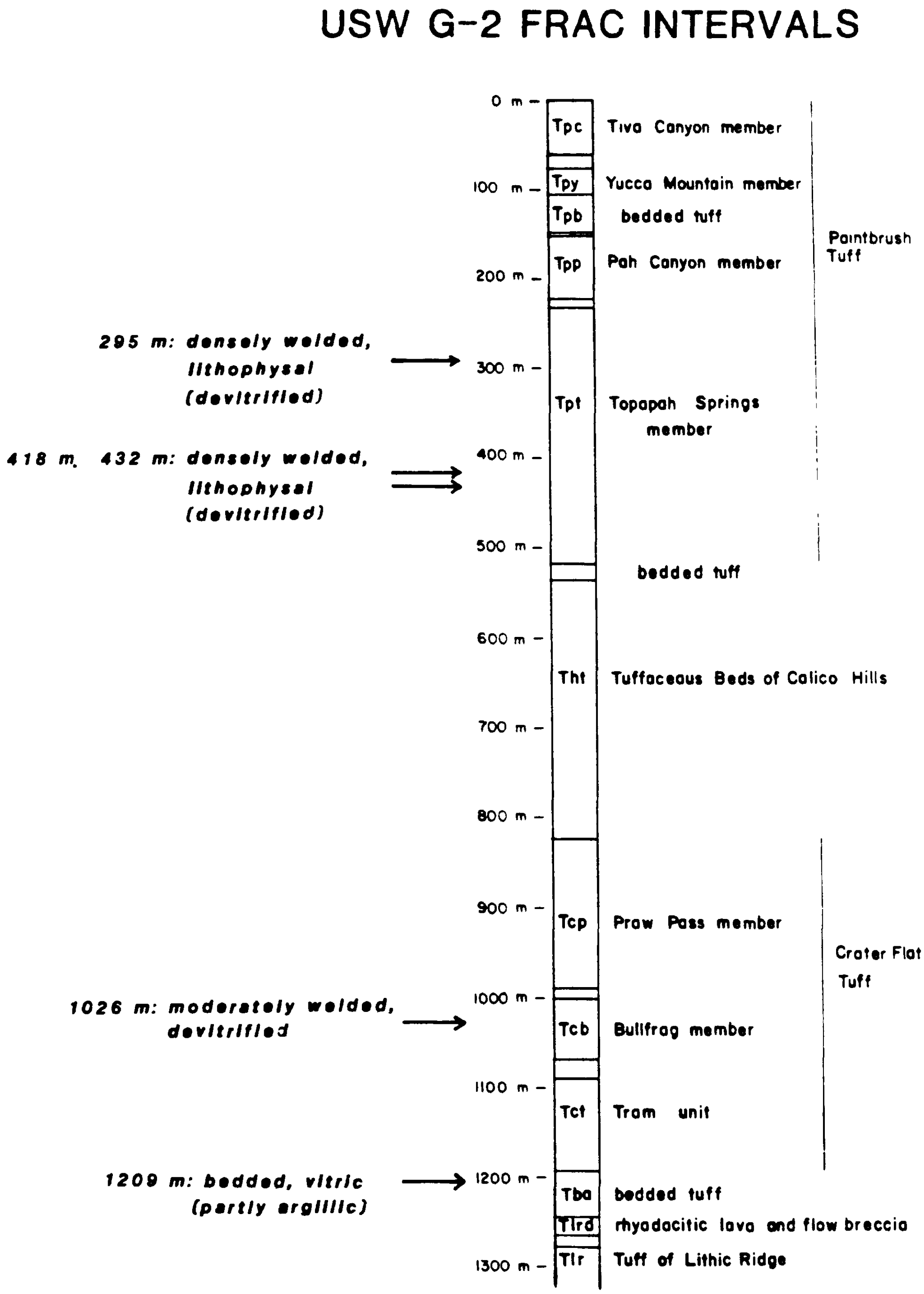

Figure 2. Stratigraphic section of hole USW G-2 and description of core (from Maldonado and Koether, 1983) for intervals of successful hydrofracture tests.

HYDROFRACTURE STRESS MEASUREMENTS - METHOD

We present a brief summary of the hydrofracture method of stress measurement used in USW G-2; interested readers are referred to Hickman and Zoback (1983) and Healy et al (1983a) for further details. An interval of the borehole (about 2.5 m long) is sealed off with cylindrical rubber packers connected through a tubing string to the surface. A pressure recorder in the tubing string just above the isolated interval is used to monitor fluid pressure throughout the test. Fluid pressure in the tubing string is controlled by pumping in (or bleeding off) fluid at the wellhead. After the packers are inflated to the desired pressure, the circulation valve in the tubing string between the packers is opened ("knockdown"), allowing the fluid pressure in the tubing string to equalize with the fluid pressure in the isolated interval. Fluid pressure in the interval is increased by constant-rate pumping at the surface until a fracture is formed ("breakdown"). The pressure-time behavior of the interval is observed over several more constant-rate pumping cycles to obtain stable, repeatable pumping pressures and instantaneous shut-in pressures (ISIPs). Finally, pumping rate is decreased in steps in order to record the equilibrium pressure for each pump rate.

Determination of Sh

Hydrofracture theory is based on the mathematical solution for the stress distribution in a homogeneous, isotropic, linearly elastic medium containing a vertical cylindrical hole. It is assumed that one principal stress direction is parallel to the borehole axis (the vertical stress, S_v) and that the other two principal stress directions are in the horizontal plane (minimum horizontal principal stress, S_h, and maximum horizontal principal stress, S_H). The theory predicts that at high enough borehole pressure, the wall rock will fail in tension, forming a vertical fracture perpendicular to S_h (Hubbert and Willis, 1957). The pressure required to hold this fracture open (the ISIP) should be equal to S_h.

For tests in which clear instantaneous shut-in pressures (ISIP's) are obscured by high formation permeabilities, the value of S_h can be verified from a plot of injection pressure vs. injection rate. This method is based on the observation that the hydrologic behavior of a hydrofractured interval changes dramatically as pressure drops and the hydrofracture closes (Earlougher, 1977). The pressure at which the fracture closes away from the wellbore (ISIP) coincides with a slope change on a pumping rate vs pressure plot. This method was used to further constrain the ISIP values for the tests at 295 m, 432 m, and 1026 m (Figure 3).

Determination of SH

Under the assumptions of hydrofracture theory, the magnitude of S_H can be calculated from the measured values of S_h, the borehole pressure required to initiate the fracture (breakdown pressure, P_b), the pore

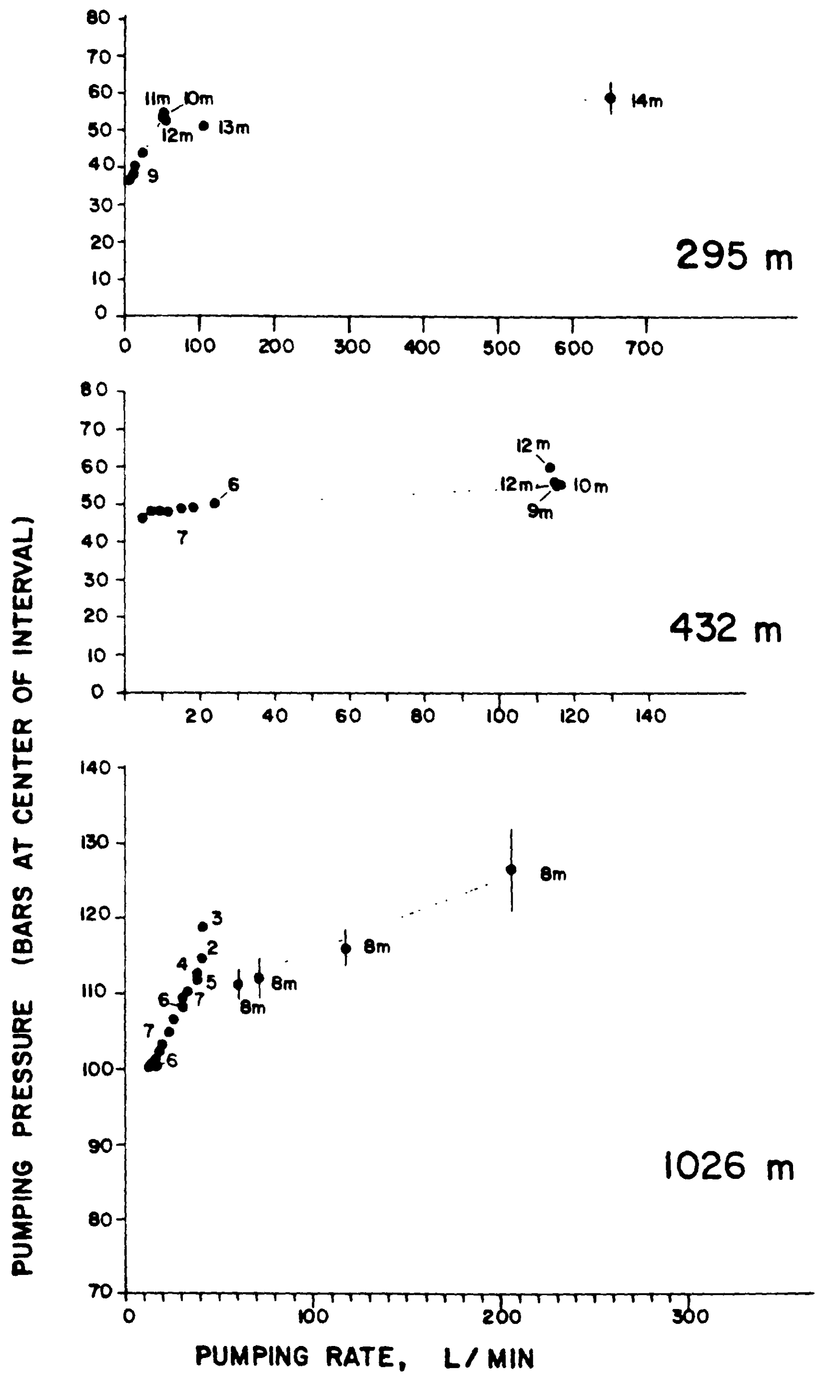

Figure 3. Plots of injection pressure vs. injection rate for three of the hydrofracture tests in USW G-2. Number of pumping cycle is shown. An "m" indicates measurement based on injection pressure of REECo mud pump, with bars indicating range of injection pressures. Change in slope of line indicates pressure at which the hydrofracture can be held open (S_h).

pressure in the rock (P_p), and the tensile strength of the rock (T). These are related by the equation (Haimson and Fairhurst, 1967):

$$P_b = 3S_h - S_H + T - P_p \quad (1)$$

If the pressure in the frac interval can be returned to its pre-frac value after the rock has been fractured, the frac reopening pressures in later cycles (P_b at T=0) can be used to determine S_H using Bredehoeft et al's (1976) modification of equation (1):

$$P_b(T=0) = 3S_h - S_H - P_p \quad (2)$$

It is generally more reliable to estimate S_H by using equation (2) than by using laboratory determinations of T in equation (1) (Hickman and Zoback, 1983). However, the unusually low water level in USW G-2 (526 m) prevented the return of pressure in the frac interval to its pre-frac value, so equation (2) could not be used to determine S_H. S_H could be calculated, however, using equation (1) if good values for P_p and T were known.

The pore pressure in saturated-zone rocks is normally calculated as the weight of a column of water from the equilibrium static water level down to the desired depth. However, if the frac interval has been exposed to abnormal fluid pressures for long periods of time, the actual value of P_p may be uncertain. This has been a problem in previous hydraulic fracturing experiments because the testing method required a long wait after the circulation valve was open before the test could begin. In the tests conducted in USW G-2, a modified equipment design allowed us to start pressurizing the interval to breakdown immediately after opening the interval to the pressure in the tubing. Because the frac interval was exposed to abnormal fluid pressure only for a very short time before the hydrofracture was created, the pore pressure should not have been significantly affected. Therefore, we have calculated pore pressure values based on the normal water level in the hole (526 m below the surface). We feel that the P_p values for USW G-2 are well enough known that they do not contribute much to the uncertainty in calculated values of S_H.

The biggest contribution to uncertainty in estimation of S_H comes from the estimate of the tensile strength, T. Tensile strengths of tuffs and flows vary widely, depending on the degree of welding and alteration. It is therefore desirable to obtain tensile strength measurements on rocks of the same unit and similar lithology as the units in the hydrofractured interval. No tensile strength determinations have been made yet on the rocks from USW G-2. However, Blacic et al (1982) determined an average tensile strength of 24 bars by Brazil test on a sample of the Bullfrog Member from USW G-1. The sample tested had similar lithologic characteristics to the Bullfrog in the frac interval at 1026 m in USW G-2. Because Brazil test tensile strength values are consistently lower than hydrofracture tensile strength values (e.g. Hudson, 1971), Blacic et al's value is used as a lower bound on the hydrofracture tensile strength. An upper bound on the tensile strength comes from the 47-bar difference between initial frac opening pressure (the breakdown pressure) and frac reopening pressure from the second cycle of this test.

Although these bounds are large, they at least provide some indication of the range of likely S_H values. This knowledge can be used qualitatively to evaluate the tectonic environment at Yucca Mountain and to distinguish between normal faulting and strike-slip faulting regimes.

Determination of Sv

The vertical stress, S_v, is equal to the saturated weight of the overlying rocks. It is an important parameter in the interpretation of stress data from USW G-2 because its magnitude influences the potential for motion along preexisting faults. Therefore, the most accurate S_v values possible should be obtained.

We calculated the S_v values listed in Table 1 by integrating commercial borehole compensated density logs of USW G-2, where good data was available (below 853 m). Densities for members of the Paintbrush Tuff above this depth were estimated from densities of the same units in nearby holes USW G-1, USW H-1, and Ue25a-1 (Snyder and Carr, 1982). In view of the lateral changes in welding and porosity that have been observed in the Paintbrush Tuff elsewhere at Yucca Mountain, we estimate that the upper part of the S_v curve may be uncertain by as much as 10%.

Equipment modifications used in tests

Previous hydraulic fracturing tests in USW G-1 (Healy et al., 1983a) had indicated the need for some special procedures because of the depth to the water table in the hole (575 m), and the tendency for the pressure in the fracture interval to drop below surface pressure during testing. USW G-2 also had a low water level (526 m), so several special procedures were tested and found to be very useful. In addition to the usual Amerada-type pressure gauge used downhole, an electronic pressure transmitter attached to the cable head was used to record pressures downhole. A rubber wireline lubricator was used to seal off the well head so that pressures above surface pressure could be maintained while the electronic pressure transmitter was providing a downhole record.

The use of the lubricator at the surface, and the decline of the water pressure below surface pressure during testing, affect the nature of the pressure-time curves. With the wellhead sealed and the water pressure above the surface hydrostatic pressure (i.e. with water completely filling the pipe), a small loss of fluid (e.g. by flow into the wall rock of the isolated interval) results in a high rate of pressure change with time. However, with the lubricator off and the pressure below the surface hydrostat, the same fluid loss causes a much lower rate of pressure change with time. The pressure at which the water level in the pipe drops below surface pressure corresponds to an inflection in the pressure-time curve (see tests at 1026 m and 1209 m, Figure 4). This inflection is not an ISIP; it merely represents the change in compliance of the system as the pressure in the pipe drops below the surface hydrostatic pressure.

Table 1. USW G-2 vertical stress calculations

interval (m)	density (gm/cm3)	source	S_v (bars)	S_v at base (bars)	Lithologic units
0 - 232	2.10	1	47.71	47.71	
232 - 277	2.17	2	9.73	57.44	Upper members of
277 - 335	1.87	2	10.62	68.06	the Paintbrush Tuff
335 - 398	2.01	2	12.32	80.38	
398 - 457	2.04	2	11.89	92.27	
457 - 518	2.00	2	11.96	104.23	
518 - 536	2.10	2	3.77	108.00	Topopah Springs
536 - 632	2.20	2	20.58	128.58	member of the
632 - 730	1.87	2	18.00	146.58	Paintbrush Tuff
730 - 826	1.90	2	17.89	164.47	
826 - 853	2.10	2	5.59	170.06	
853 - 884	2.35	3	7.03	177.09	
884 - 914	2.30	3	6.88	183.97	Tuffaceous Beds
914 - 945	2.16	3	6.46	190.43	of Calico Hills
945 - 975	2.20	3	6.58	197.01	
975 - 1006	2.20	3	6.58	203.59	
1006 - 1036	2.30	3	6.88	210.47	Prow Pass member of
1036 - 1067	2.26	3	6.76	217.23	Crater Flat Tuff
1067 - 1097	2.24	3	6.70	223.93	
1097 - 1128	2.34	3	-7.00	230.93	Tram member of
1128 - 1158	2.15	3	6.43	237.36	Crater Flat Tuff
1158 - 1189	2.18	3	6.52	243.88	
1189 - 1219	2.31	3	6.91	250.79	bedded tuff, lava,
1219 - 1241	2.42	3	5.06	255.85	and flow breccia

Sources of density information:
(1) estimated from various values reported in Snyder and Carr (1982)
(2) values for units in USW H-1 (Snyder and Carr, 1982)
(3) integration of Dresser-Atlas borehole compensated density log, USWG-2

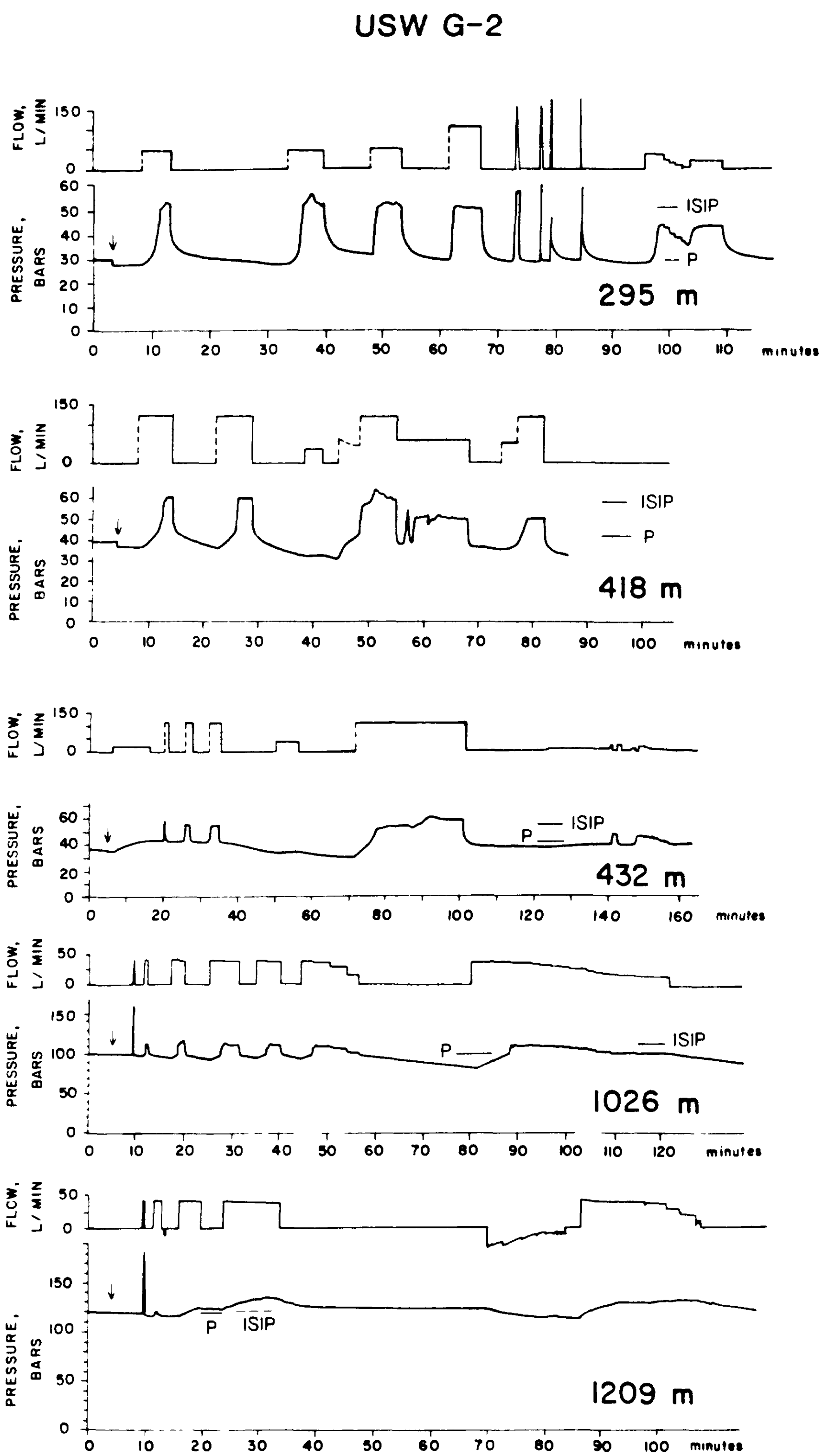

Figure 4. Pressure and flow rate vs. time for 5 successful hydrofracture tests in USW G-2. Arrows indicate the time at which the circulation valve was opened, so that the hydrofracture interval was exposed to the pressure in the tubing string. The upper 3 tests were conducted above the water level in the hole, and the drop in pressure following the opening of the circulation valve results from water rushing in to replace the air in the test interval. ISIP = value of S_h obtained from test; P = surface hydrostatic pressure.

HYDROFRACTURE STRESS MEASUREMENTS - RESULTS

A total of 13 hydrofracture tests were attempted in USW G-2, at depths between 295 m (969 ft) and 1209 m (3966 ft) (Table 2). The shallowest four tests were conducted in the unsaturated zone. Of all the tests, five yielded good data on the value of the least horizontal principal stress, S_h (Table 3 and Figure 4). One test failed due to packer leakage, and the other seven did not constrain S_h well enough to be considered good data.

In spite of the equipment modifications to deal with the low water level in USW G-2, the general behavior of the USW G-2 rocks during testing was extremely unusual. In most hydrofracture testing, including the work in USW G-1, pumping rates less than 40 l/min are sufficient to conduct the entire test. Such pumping rates were sufficient to conduct good hydrofracture tests in the lower portion of USW G-2 (tests at 1026 m and 1209 m, Figure 4 and Tables 2 and 3), but proved to be insufficient for tests higher in the hole. As this problem became apparent during testing, a mud pump was borrowed from REECo in order to achieve higher pumping rates (up to 150 l/min). The rate of fluid flow required to conduct the three good tests in the upper portion of the hole (295 m, 418 m, 432 m) was larger than encountered in normal hydrofracture testing.

The hydrofracture tests at 295 m, 418 m, and 432 m showed good, repeatable pumping pressures, with the same frac opening pressure on the first cycle as on later cycles (Figure 4). This suggests either that we were pumping into a preexisting fracture, or that we were creating a new hydrofracture in a formation which had zero tensile strength. The high pumping rates accepted by the fractures at 418 and 432 m on all cycles (125 l/min, Figure 4) suggests that, rather than creating new hydrofractures, we were tapping into fairly extensive preexisting fracture systems. The flow rates needed in the test at 295 m are closer to typical flowrates, but the general character of the pressure-time curves suggests that possibly a smaller preexisting fracture was being reopened in this test.

If preexisting fractures were being reopened, then it is important to know the orientation of these fractures in order to understand how the ISIPs measured during the test are related to the value of S_h. A fracture that is not perpendicular to S_h will have an ISIP that exceeds the true value of S_h. Because no televiewer photos could be obtained above the water table, we do not have good information on number and orientation of preexisting fractures in these intervals in the unsaturated zone. However, downhole television logs show preexisting fractures close to all except the deepest test interval in the unsaturated zone, and televiewer logs below the water table show that the preexisting fractures lower in the hole are generally oriented perpendicular to S_h (see Appendix). Because of the consistency of the fracture orientations in the upper part of the televiewer log, it is likely that the shut-in pressures measured by these tests represent values very close to S_h. However, it cannot be proven, so we have indicated in Table 3 that the measured ISIPs are upper bounds on the value of S_h for the three tests in the unsaturated zone.

Table 2. Summary of hydrofracture attempts, NTS USW G-2

Depth	Result	S_h (bars)	date
969 ft (295 m)	Stable pressures after knockdown. First cycle frac open same as on later cycles; interpreted to represent opening of preexisting fracture. S_h from ISIPs confirmed by pump test data.	≤ 51±1	11/05/82
1265 ft (386 m)	See some sort of fracture but not enough pump rates to determine S_h.	--	11/03/82
1371 ft (418 m)	Reopening preexisting fracture. S_h based on repeatable pumping pressures.	≤ 54±1	11/04/82
1416 ft (432 m)	Reopening preexisting fracture. S_h based on repeatable pumping pressures from first 3 cycles.	≤ 55±1	11/02/82
1907 ft (581 m)	One stable pump pressure. No clear opening pressure of fracture observed.	--	11/01/82
1940 ft (591 m)	Two cycles, no clear fracture opening pressure observed.	--	10/26/82
2362 ft (720 m)	Sharp pressure drop at knockdown.	--	10/22/82
2398 ft (731 m)	Sharp pressure drop at knockdown. Not enough resolution in pressure to see a knee in the pressure-time curve.	--	10/18/82
2478 ft (755 m)	Sharp pressure drop at knockdown. Not enough resolution in pump cycles to identify S_h.	--	10/12/82
2658 ft (810 m)	Sharp pressure drop at knockdown. Not enough resolution in pump rates to identify S_h.	--	11/03/82
3365 ft (1026 m)	Clear breakdown and repeatable fracture reopening pressures. S_h from ISIP and confirmed by pump rate vs. pressure plots.	111±2	10/13/82
3706 ft (1130 m)	Packer leak, no results.	--	10/25/82
3966 ft (1209 m)	Clear breakdown pressure. Behavior changes after cycle 2, as if fracture has intersected a large preexisting fracture system. S_h based on behavior of first two cycles.	120±2	10/20/82

TABLE 3. SUMMARY OF STRESS MEASUREMENTS, USW G-2

Depth (m)	Breakdown Pressure (bars)	Shut-in Pumping Pressure (bars)	Hydrostatic Pressure (bars)	Pore Pressure[2] (bars)	S_h (bars)	S_v[3] (bars)	T (bars)	S_H (bars)	Comments
295	51 ± 1[1]	51 ± 1	29	0	$\leq 51 \pm 1$	61			Reopening preexisting fracture of unknown orientation; shut-in pumping pressure is upper bound on S_h.
418	54 ± 1[1]	54 ± 1	41	0	$\leq 54 \pm 1$	84			Same as above.
432	55 ± 1[1]	55 ± 1	42	0	$\leq 55 \pm 1$	87			Same as above.
1026	163	111 ± 2	101	49	111 ± 2	208	35 ± 12	156 ± 18	Minimum horizontal stress from stable pumping pressures on multiple cycles.
1209	182	120 ± 2	118	67	120 ± 2	255			Minimum horizontal stress from flat pumping pressure attained on second cycle.

1. No clear breakdown pressures seen; see comments column and Figure 4.
2. Based on water table at 526 m depth.
3. Based on densities and calculations in Table 1.

The other hydrofracture test in the unsaturated zone (386 m) was unsuccessful and showed unusual behavior in that first-cycle pressure, at 100 l/min pump rate, rose rapidly to 70 bars and then remained steady, as if a fracture were being opened and pressurized. However, on subsequent cycles at lower pump rates (40 l/min or less), this fracture opened at 49-45 bars and the pressure immediately decayed rapidly, even during pumping. Such rapid pressure drops prevent determination of the ISIP and suggest that the fracture being opened is in comunication with the open hole above or below the isolated interval.

Two unsuccessful tests at 581 m and 591 m also failed to show clear breakdown pressures or clear fracture reopening pressures, despite high pump rates (110 l/min). Because of the high apparent permeabilities, the long pumping times required, and the characteristics of buildup and decay of these pressure curves, we believe that these tests were communicating with the open hole rather than testing a closed fracture system. Possibly, the packers may have failed to isolate the frac interval. Smaller, undetected fractures within the isolated interval might have permitted fluid flow past the packers and into the surrounding hole.

The next four unsuccessful tests (at 720 m, 731 m, 755 m, and 810 m) had one very curious feature in common; they all showed a rapid pressure drop of very large magnitude (15 - 20 bars) when the circulation valve was opened, suggesting that the pressure in the pipe at knockdown, although no greater than the surface hydrostat, was too high to be held by the interval. This pressure at knockdown may either have opened a preexisting fracture of arbitrary orientation, or created a new hydrofracture. Because interval pressurization up to breakdown was not observed, and because we did not have access to the REECo mud pump for the higher flow rates necessary during these tests, these tests did not yield enough information to be used in our interpretation. We feel that for the six tests between 581 m and 810 m, the most likely explanation for the inconclusive results of the tests is that the formation was somehow fractured by setting the packers, so that fluid in the interval could flow out and connect with the fracture systems leading to the open hole. This would explain both the very high pumping rates needed to produce any pressure change in the interval, and the character of the pressure decay curves from these tests.

Two of the lowest hydrofracture tests in USW G-2 (at 1026 m and 1209 m) showed good breakdown pressures and were considered to be quite good tests (Figure 4). The test at 1026 m had repeatable stable pumping pressures which gave a good value for S_h and allowed estimation of S_H as well, using equation (1). The test at 1209 m exhibited two-stage behavior, with pumping pressures rising significantly after cycle 2, as if the frac had intersected a preexisting fracture system or large impermeable cavity. The S_h value inferred from this test is based on the pressure behavior of the fracture during the first two cycles. S_H was not estimated for this test because of lack of tensile strength information for the rock unit in the tested interval (discussed below).

DISCUSSION

All five S_h values obtained at USW G-2, and the one S_H value estimated, are less than the vertical stress (Table 1 and Figure 5). These measurements indicate that at the depths tested, the tectonic stress field corresponds to a normal faulting regime. We did not estimate S_H for the three shallower tests (295 m, 418 m, 432 m) because of the possibility that the fractures were not optimally oriented perpendicular to S_h, and that the ISIPs of these tests may be only upper bounds on the value of S_h.

As of this report, hydrofracture tests have been performed in two other holes at Yucca Mountain: USW G-1 (Healy et al, 1983a) and UE25p-1 (Healy et al, 1983b). The measurements in holes USW G-1 and USW G-2 show a similar pattern of S_h vs. depth (Figure 6). No good S_H values were obtained for USW G-1 because of lack of precise tensile strength information; however, for S_H to exceed S_v in USW G-1, unreasonably high values of tensile strength (in excess of 65 bars) would be required. Therefore, both USW G-1 and USW G-2 are interpreted to have relative stress magnitudes indicative of a normal faulting regime (i.e., S_v is larger than both S_H and S_h).

As discussed by Healy et al (1983a), USW G-1 is very close to failure by normal faulting on optimally oriented preexisting normal faults. This appears to be the case for USW G-2 as well. Frictional sliding on preexisting faults optimally oriented to the stress field will occur at a ratio of stresses controlled by the coefficient of friction, μ, and the pore pressure, P_p. In a normal faulting regime, frictional sliding can be expected on optimally oriented faults whenever the ratio of $(S_v - P_p)/(S_h - P_p)$ exceeds the value $((\mu^2 + 1)^{1/2} + \mu)^2$ (Zoback et al., 1978). For reasonable values of u (between 0.6 and 1.0; Byerlee, 1978) the values of S_h determined in USW G-2 are close to those at which frictional sliding might be expected to occur on high-angle faults of N25°E to N30°E strike (Figure 7).

Preliminary analysis of one stress measurement in tuff in hole UE25p-1 (Healy et al, 1983b) indicates much higher stresses for that hole than for USW G-1 or USW G-2 (Figure 6). Hole UE25p-1 appears to be under stable stress conditions, and have relative stress magnitudes characteristic of a strike-slip or thrust faulting regime. The cause of such a large lateral variation in magnitudes of principal stresses is not yet understood; further stress studies in the vicinity of Yucca Mountain may help to resolve this problem.

BOREHOLE TELEVIEWER STUDIES - METHOD

The principle of borehole televiewer measurements has been described by Zemanek et al (1970) and is only briefly summarized here. The borehole televiewer is an acoustic transducer which emits 2 MHz pulses at a rate of 1800/sec. It rotates 3 times per second and is pulled up the hole at 2.5 cm/sec. The reflected signal is continuously recorded on magnetic tape, and its amplitude and arrival time can be used to

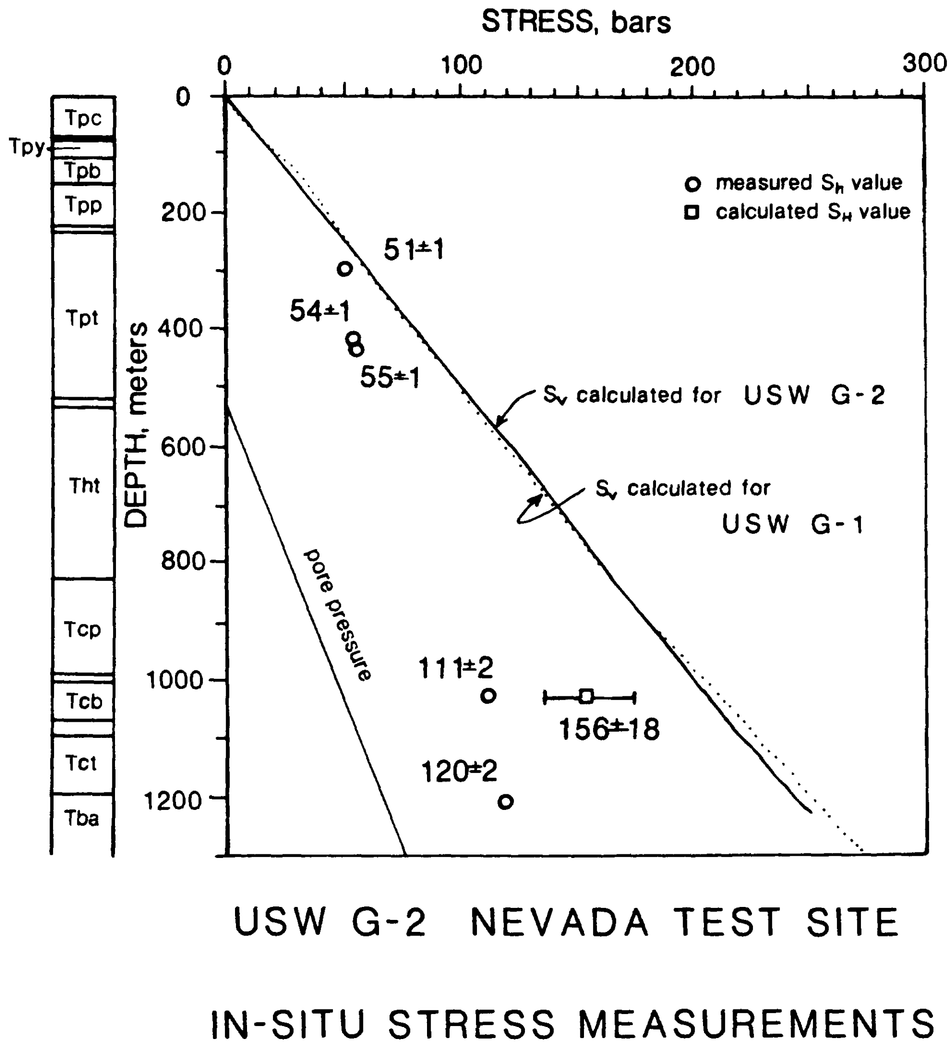

Figure 5. Summary diagram of stress vs. depth in USW G-2. The stratigraphic section is from Figure 2.

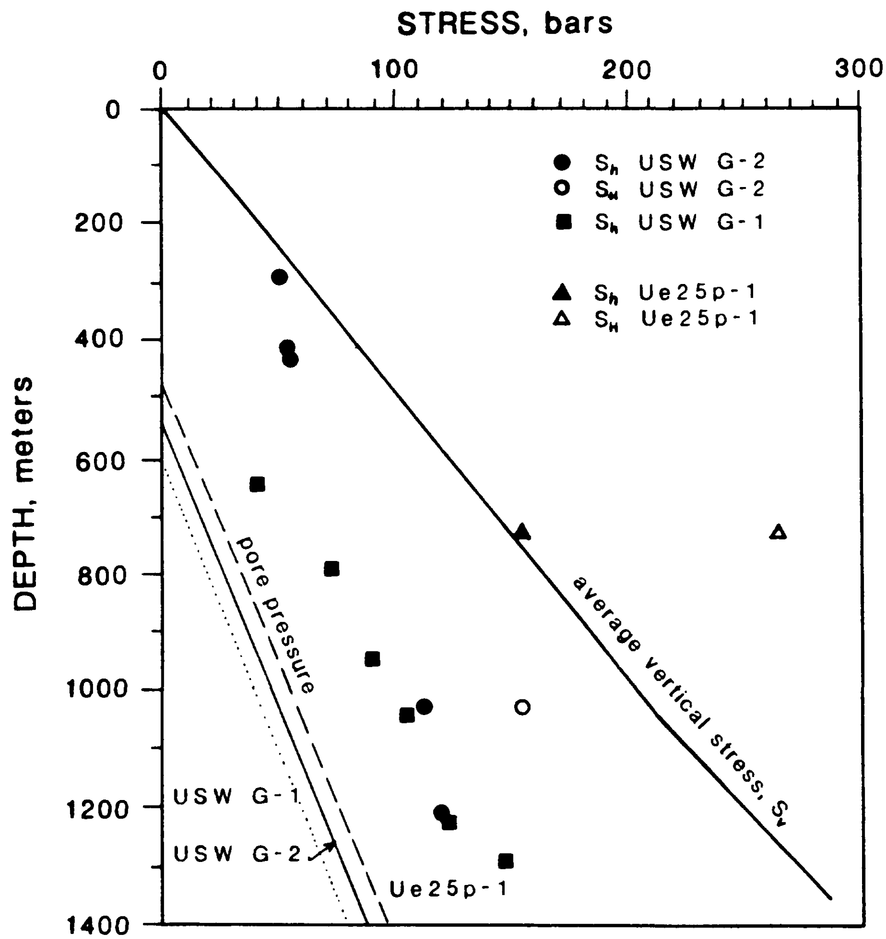

COMPARISON OF STRESS MEASUREMENTS,
HOLES USW G-1, USW G-2, Ue25p-1
YUCCA MOUNTAIN, NEVADA

Figure 6. Least horizontal principal stress values (S_h), lithostatic pressure (S_v), and pore pressure plotted against depth for the three holes tested at Yucca Mountain. Note that the values obtained for USW G-1 and USW G-2 show a very similar trend, whereas those for Ue25p-1 indicate a different state of stress.

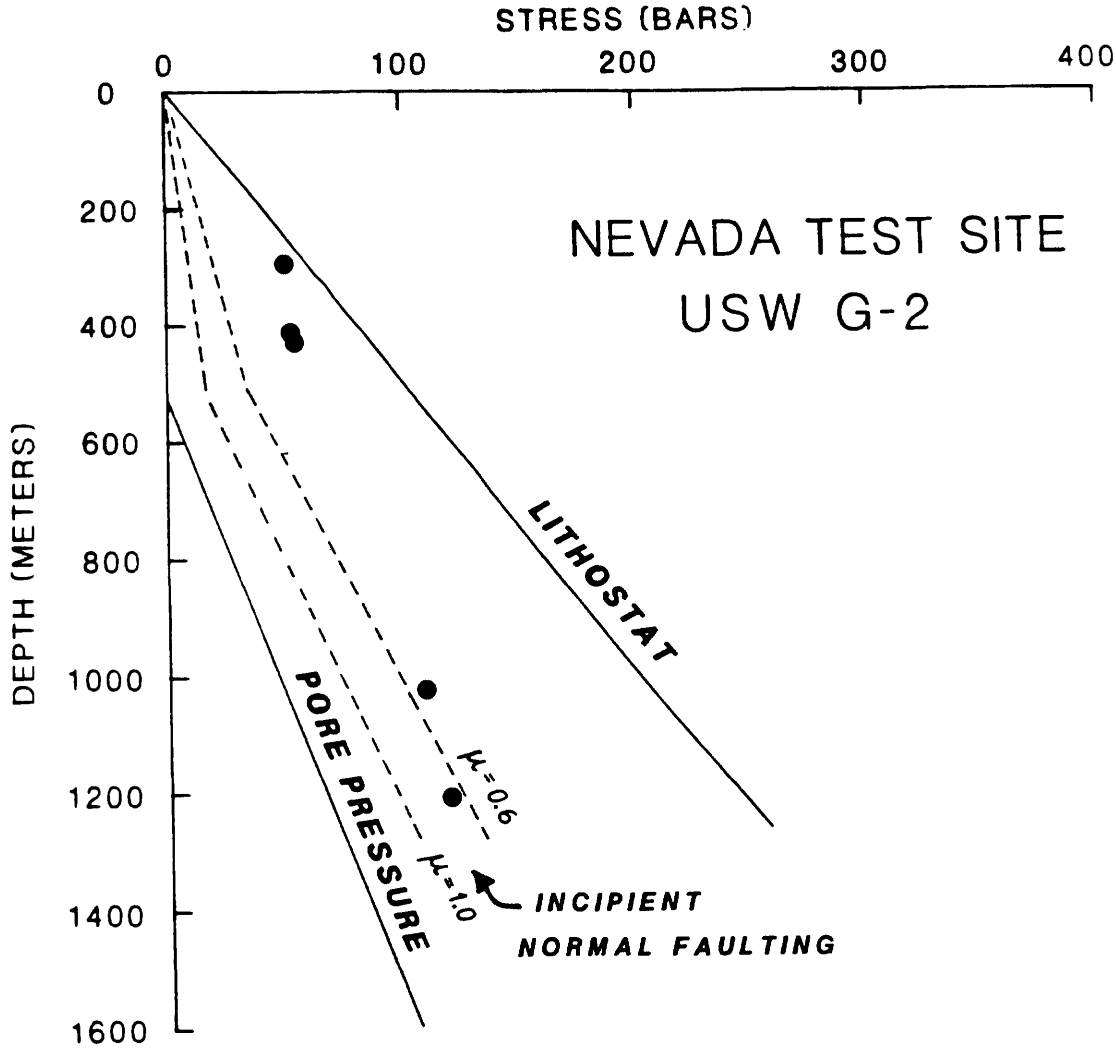

Figure 7. Least horizontal principal stress values for USW G-2, plotted against depth. Lithostatic pressure (S_v) and pore pressure (based on depth of 526 m to the water level in the hole) are also shown. Stress values falling to the left of the dashed lines correspond to those for which slip might be expected to occur on preexisting optimally oriented normal faults, for reasonable values of the coefficient of friction, μ (0.6 to 1.0).

determine both the smoothness of the borehole wall and the cross-sectional shape of the borehole.

For typical televiewer logs, the amplitude of the reflected signal is plotted as brightness on a three-axis oscilloscope, as a function of beam azimuth and vertical position in the hole. The scope trace is triggered at magnetic north by a flux-gate magnetometer, to provide a reference for the azimuth of observed features. The oscilloscope display is photographed to make a continuous record of the data and permit identification of lithologic characteristics, fault zones, and stress-related features such as fractures and breakouts. Such features typically cause a decrease in amplitude of reflected signal due to increased roughness of the borehole wall and consequent greater scattering of reflected signal away from the receiver.

Dipping planar features such as fractures appear as dark sinusoidal bands on the televiewer photos (Figure 8). Because a single 360° sweep is pictured on each horizontal trace, the amount of vertical distortion of these features depends on borehole diameter and logging speed. In USW G-2, average borehole diameters of 23 cm above 814 m depth and 18 cm below caused horizontal exaggeration of 2.8:1 and 2.1:1, respectively. This improved the resolution of steeply dipping features but made the detection of shallowly dipping features more difficult. Resolution was also affected by formation reflectivity, smoothness of the wellbore, and acoustic impedance of the wellbore fluid.

BOREHOLE TELEVIEWER STUDIES - OBSERVATIONS

The televiewer log of USW G-2 was recorded from a depth of 1250 m (4100 ft) to the top of fluid at 526 m (1725 ft). Distinctive features observed include throughgoing low- and high-angle fractures; very high-angle fractures which are not throughgoing and have a uniform orientation; and dark bands which represent wellbore breakouts (Appendix).

The throughgoing fractures in the televiewer photos have a preferred direction of strike from N10°E-N40°E (Figures 9, 10). This preferred orientation is weaker in the lower part of the televiewer log. The average dip of these throughgoing fractures decreases with depth. Many of these throughgoing fractures are also observed in the core and are inferred to have been present prior to drilling of the hole. Virtually all of them strike NW to NE, consistent with surface fault patterns of NW to NE trending faults on Yucca Mountain (Figure 1).

Sets of very high angle (80° to vertical dip), non-throughgoing fractures are also seen in parts of the USW G-2 televiewer log. These are parallel and tend to merge into one another along an azimuth of N25°E to N30°E. Such fractures are especially common at depth intervals of 526-532 m (1725-1745 ft), 541-570 m (1775-1870 ft), and 648-678 m (2125-2225 ft). Many of these fractures are not seen in the core. For example, the section of core from 647 m (2123 ft) to 675 m (2213 ft) contains no fractures (Scott and Spengler, 1982). The televiewer log of this same section of hole shows a series of high-angle

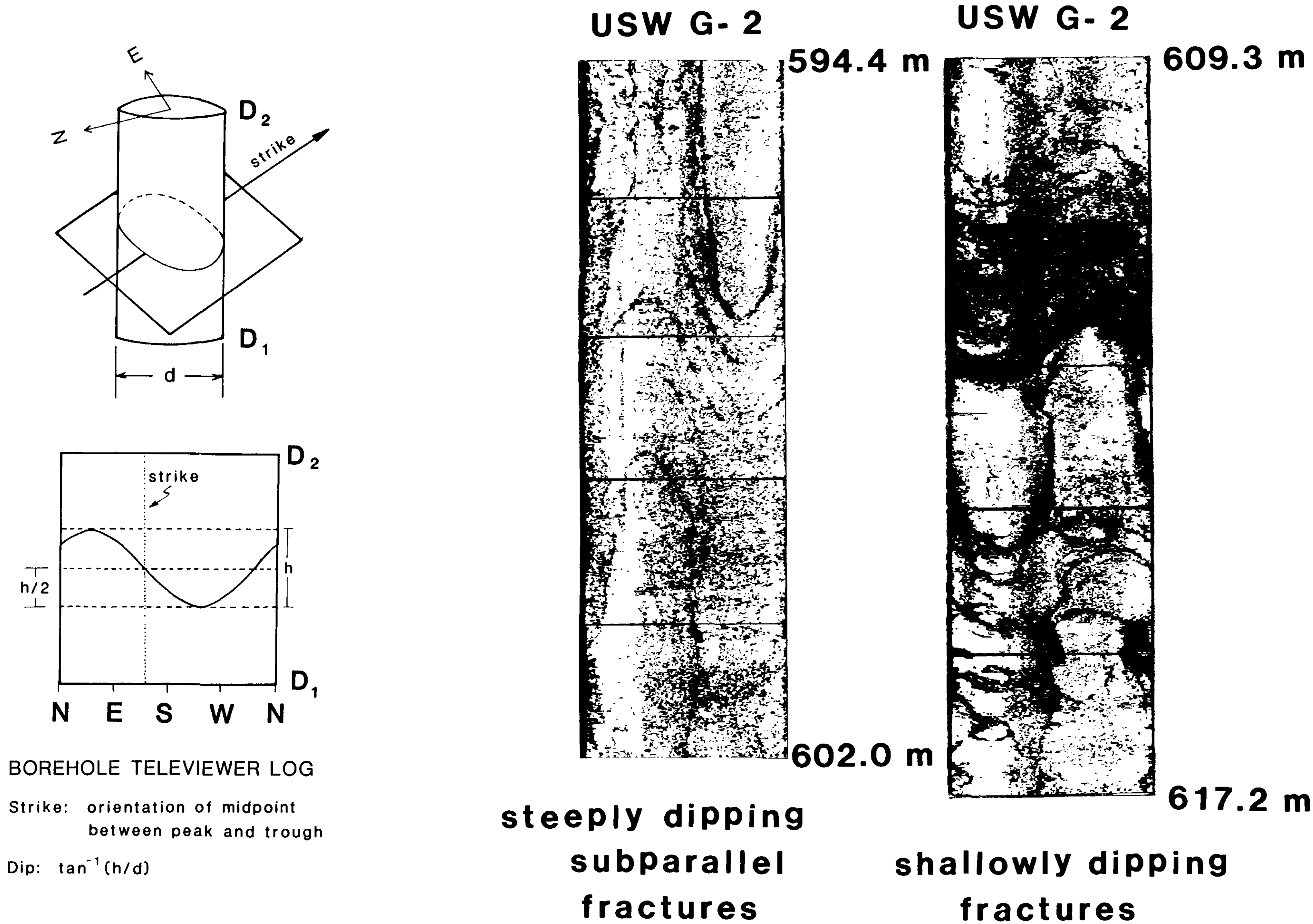

Figure 8. Example of determination of strike and dip of planar feature observed in televiewer log, with some examples of fractures observed in the USW G-2 televiewer log.

THROUGHGOING FRACTURES

SEEN IN TELEVIEWER LOG, USW G-2

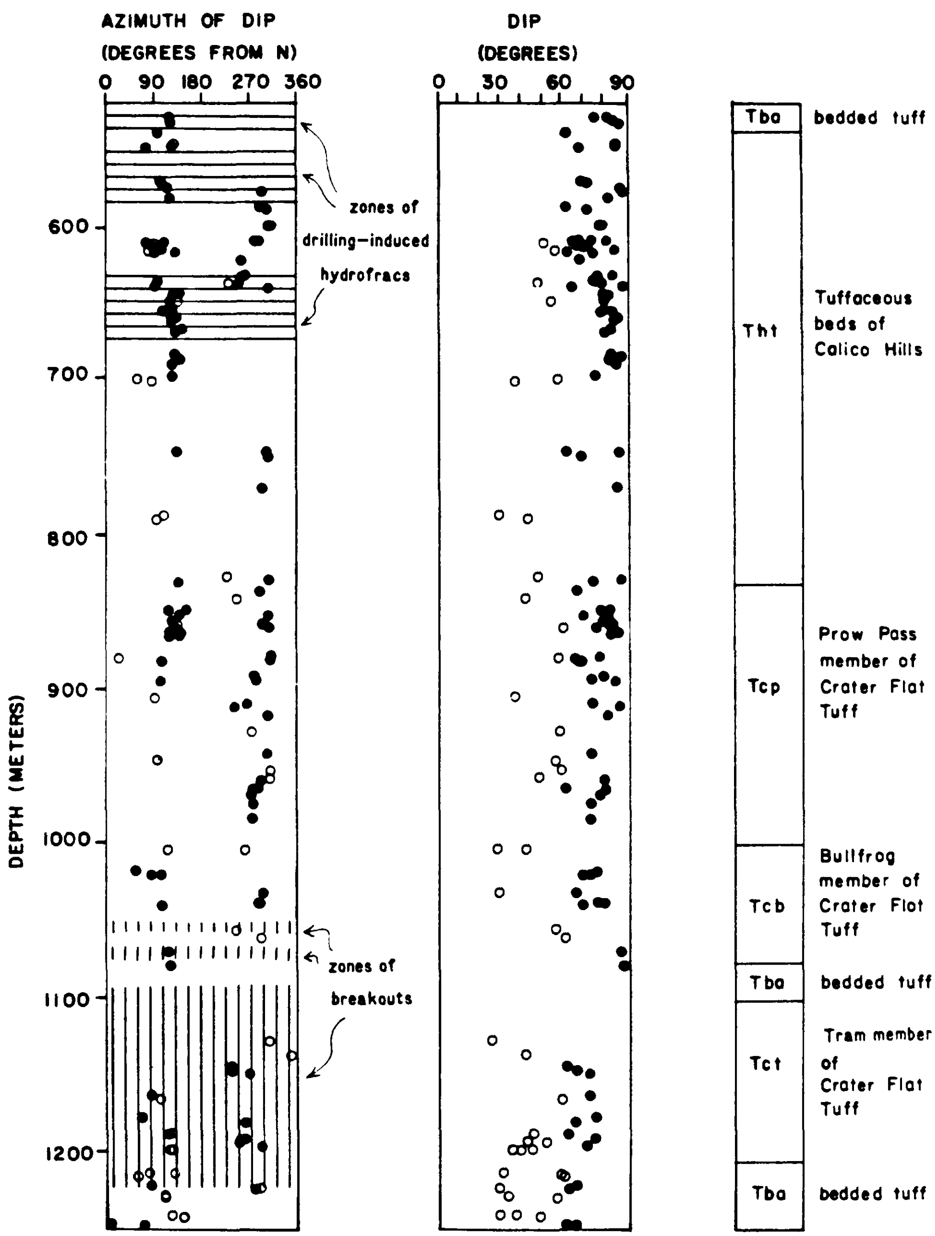

Figure 9. Plot of azimuth and angle of dip vs. depth for the throughgoing fractures observed in the USW G-2 televiewer log. The open circles represent fractures which dip less than 60°; filled circles represent fractures which dip 60° or more.

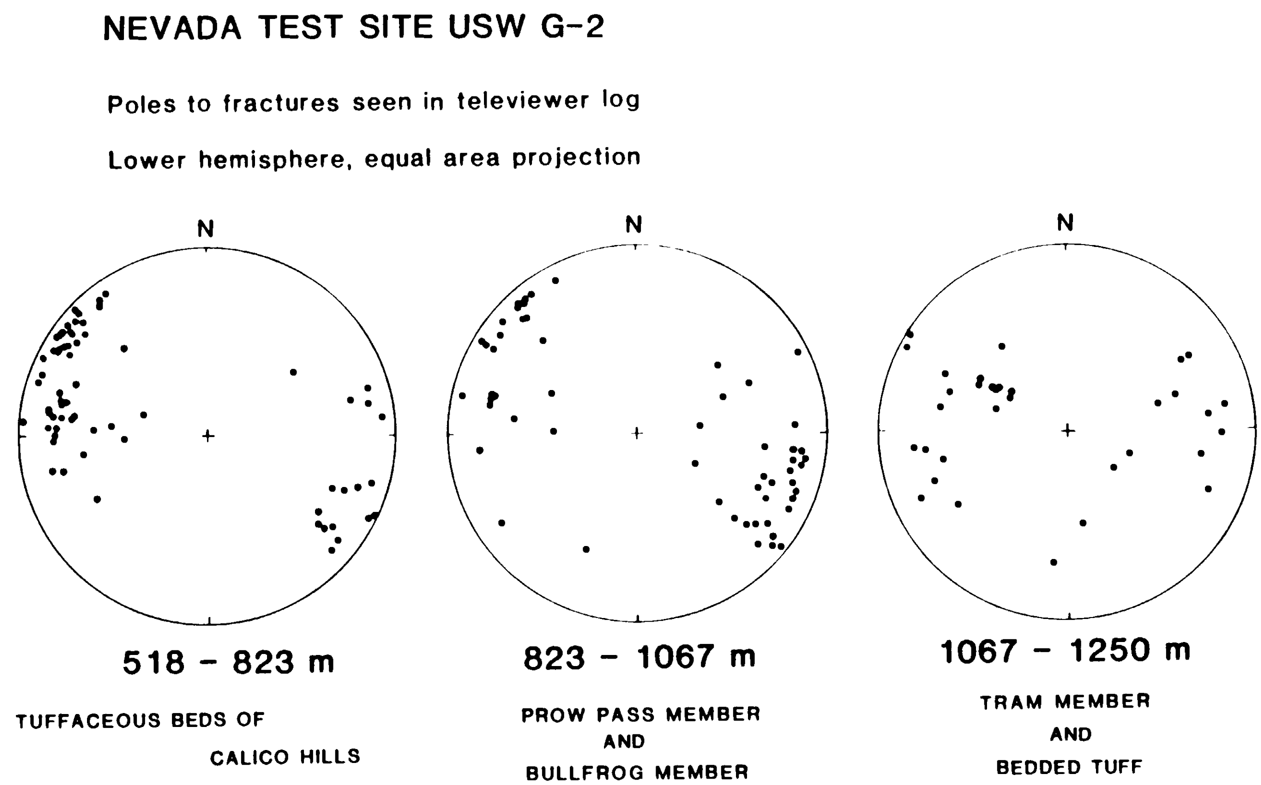

Figure 10. Lower hemisphere, equal area projections of poles to the throughgoing fractures observed in the USW G-2 televiewer log. Note the change in fracture orientations and preferred orientation with depth.

fractures of consistent strike. Because of the consistent azimuth of these features, and because they are not present in the core, they are interpreted to be hydrofractures which were caused by drilling. Such fractures are expected to extend and propagate when the fluid pressure in them exceeds S_h. During drilling, pore pressure in USW G-2 could easily have exceeded the low observed values of S_h, as the hole was filled to the surface with fluid and downhole pumping pressure was applied (Figure 11). The complete loss of circulation fluid experienced during drilling can best be explained by the fluid going out into these hydraulic fractures. Since vertical hydrofractures theoretically form normal to the direction of least horizontal principal stress, these features indicate an S_h direction of N60°W-N65°W for USW G-2.

Wellbore breakouts are also observed in the televiewer log, at depths of 1053 - 1056 m (3455 to 3465 ft), 1074 m (3525 ft), and 1084 - 1219 m (3555 to 4000 ft). In the televiewer log, these features appear as jagged, irregular black bands of consistent azimuth. Reprocessing of the televiewer log in a travel-time mode shows that these features coincide with regions of unusually large hole diameter, or "breakouts" (Figure 12). These are believed to form by shear failure of the hole wall in regions of concentrated high compressive stresses, centered on the azimuth of S_h (Bell and Gough, 1979; Zoback et al, 1982). The breakouts seen in USW G-2 have an average azimuth of about N60°W (Figure 13), suggesting that this is approximately the direction of least horizontal principal stress. Breakouts parallel to the azimuth of S_h as determined from hydrofracturing tests in the same well have also been reported from a 5250 ft deep well in central New York State (Hickman et al, 1982).

When all the hydrofracture tests were completed, the televiewer log was repeated in 20 ft sections centered on each of the tested intervals, to locate test-induced hydrofractures. No test-induced hydrofractures were observed; in all cases the post-frac televiewer photos look just like the same sections on the pre-frac televiewer log. This is not surprising, because thin closed fractures do not show up well on televiewer photos. We decided not to spend money and time running impression packers in the test intervals, because the orientations of the drilling-induced hydraulic fractures and breakouts seen in the televiewer log provide ample and clear evidence of the orientation of the current stress field.

SUMMARY

Hydraulic fracturing stress measurements in hole USW G-2 yielded low values of the least horizontal principal stress (S_h) relative to the vertical stress (S_v). Three measurements in the unsaturated zone constrain S_h there to be less than S_v. Two measurements below the water table give values of S_h which are significantly lower than S_v and which require the greatest horizontal principal stress (S_H) to be the intermediate stress, indicating that USW G-2 is in a normal faulting stress regime. The measured S_h magnitudes are close to those at which frictional sliding might be expected to occur on optimally oriented preexisting faults.

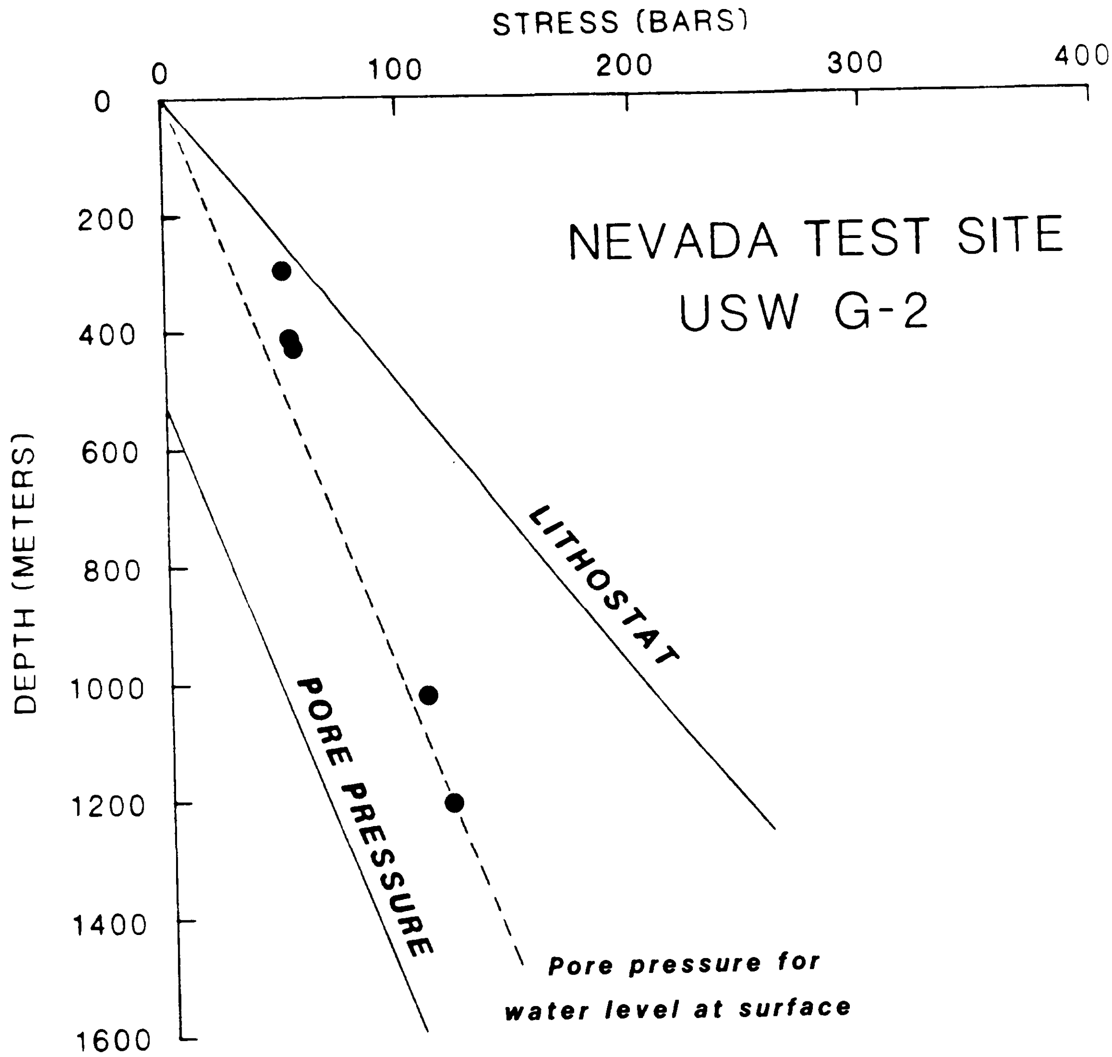

Figure 11. Measured values of least horizontal principal stress (S_h) vs. depth in USW G-2. Pore pressure line corresponding to the observed water level in the hole (526 m) is shown for reference. The dashed line is the pore pressure curve which would be expected if the hole were filled to the surface with water. The measured values of S_h suggest that the pore pressure in the hole may have exceeded S_h during drilling, causing drilling-induced hydraulic fractures to form and propagate.

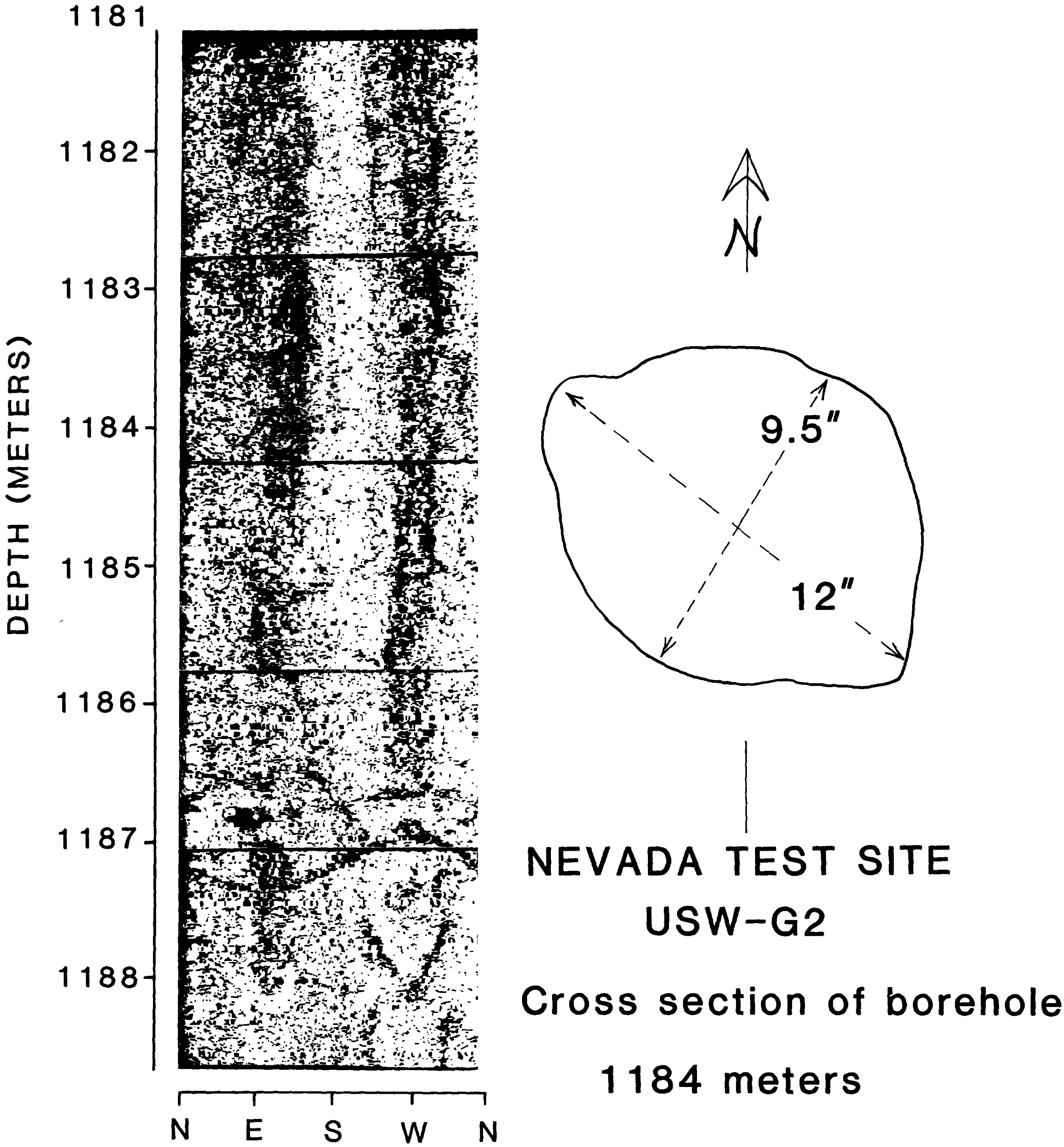

Figure 12. Typical breakout in USW G-2 showing appearance on televiewer log as a set of jagged black vertical bands. When the televiewer signal is reprocessed to make a cross-section of the hole, the black bands are seen to correspond to regions of unusually large hole diameter ("breakouts").

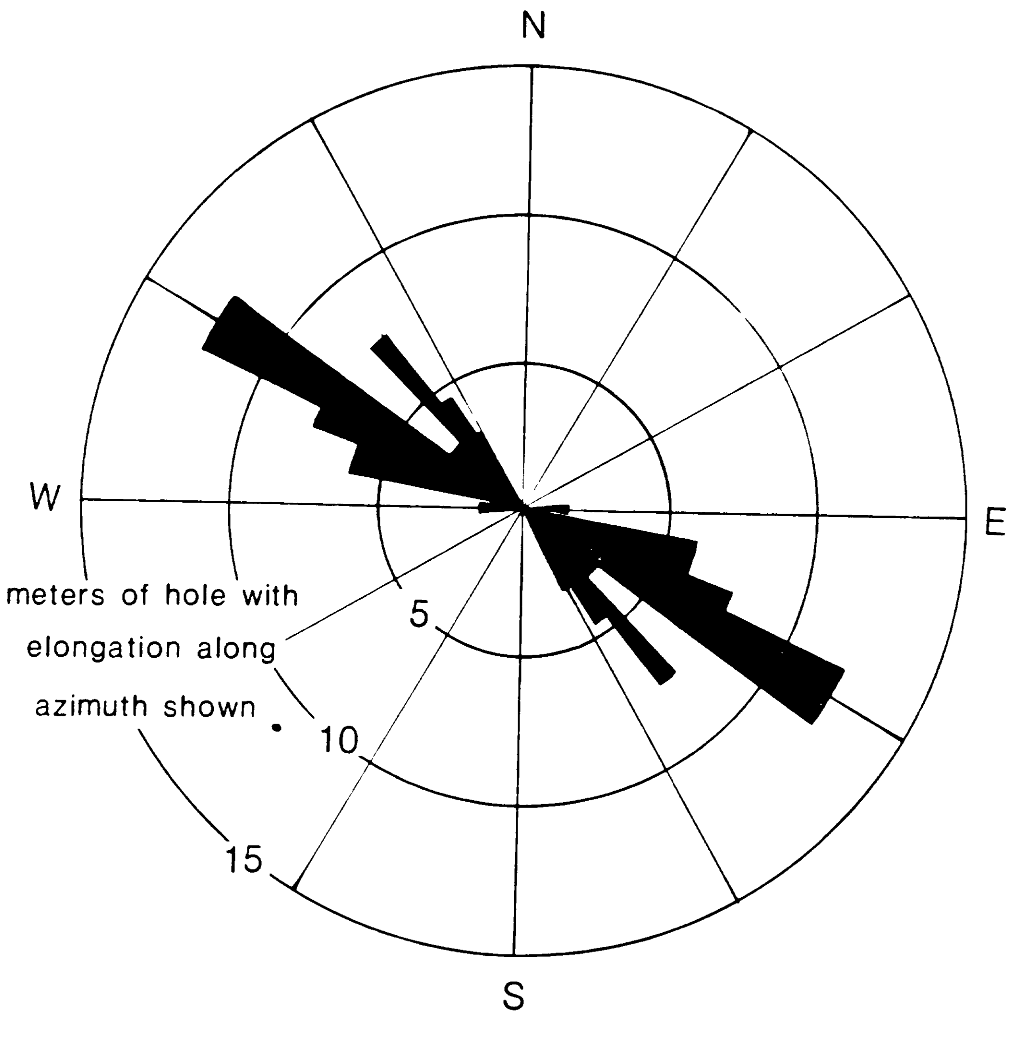

AZIMUTHS OF BREAKOUTS, NTS USW G-2

1075 - 1218 M DEPTH

Figure 13. Histogram of the orientations of breakouts, averaged over each 1.5 m interval in USW G-2.

An important feature of hole USW G-2 was the tendency for the rocks to fail in tension by the addition of very small excess pressures (such as the 52 bar excess pressure generated by filling the hole from the static water level, at 526 m depth, to the surface). Because of the low stresses acting on the area, and the low strengths of the tuffs and flow units, merely filling the hole with water was sufficient to hydrofracture the rock in much of the hole. Many such fractures, apparently induced during drilling, can be seen clearly in the televiewer photos (Appendix).

Preexisting natural fractures seen in the USW G-2 televiewer log have a preferred strike of N10°E to N40°E, similar to the strike of mapped faults in the vicinity. Observation of the azimuths of drilling-induced fractures together with stress-induced breakouts suggests a consistent orientation of N60°W to N65°W for the direction of least horizontal principal stress in USW G-2. Both this stress direction and the magnitudes of S_h determined from hydrofracture testing in USW G-2 agree very closely with observations from hole USW G-1 at Yucca Mountain.

REFERENCES CITED

Anderson, Lennart A., 1981, Rock property analysis of core samples from the Yucca Mtn. UE25a#1 borehole, Nevada Test Site, Nevada, USGS Open-File Report #81-1338.

Bell, J.S., and D.I. Gough, 1979, Northeast-southwest compressive stress in Alberta: evidence from oil wells, Earth Planet. Sci. Lett., 45, 475-482, 1979.

Blacic, J., J. Carter, P. Halleck, P. Johnson, T. Shankland, R. Andersen, K. Spiocchi, and A. Heller, 1982, Effects of long-term exposure of tuffs to high-level nuclear waste repository conditions, Preliminary Report LA-9174-PR, Los Alamos National Laboratory.

Bredehoeft, J. D., R. G. Wolff, W. S. Keys, and E. Shuter, 1976, Hydraulic fracturing to determine the regional in-situ stress field, Piceance Basin, Colorado, GSA Bulletin 87, 250-258.

Byerlee, J. D., 1978, Friction of rocks, Pure and Applied Geophysics, 116, 615-626.

Earlougher, Robert C., Jr., 1977, Advances in Well Test Analysis, AIME Monograph 5, American Institute of Mining, Metallurgical, and Petroleum Engineers, Dallas, Texas.

Haimson, B. C., and C. Fairhurst, 1967, Initiation and extension of hydraulic fractures in rock, Soc. Petr. Engrs. J., 7, 310-318.

Healy, J. H., S. H. Hickman, M. D. Zoback, and W. L. Ellis, 1983a, Report on televiewer log and stress measurements in core hole USW-G1, Nevada Test Site, USGS Open-File Report, in preparation.

Healy, J., J. Stock, J. Svitek, and S. Hickman, 1983b, Hydrofrac stress measurements on Yucca Mountain, Nevada, EOS Trans. AGU, 64, 320.

Hickman, S. H., J. H. Healy, M. D. Zoback, J. E. Svitek, and J. E. Bretches, 1982, In situ stress, borehole elongation, and natural fracture distribution at depth in central New York state, EOS Trans. AGU, 63, 1118.

Hickman, S. H., and M. D. Zoback, 1983, The interpretation of hydraulic fracturing pressure-time data for in-situ stress determination, in Hydraulic Fracturing Stress Measurements, National Academy Press, Washington, D. C., pp. 44-54.

Hubbert, M. K., and D. G. Willis, 1957, Mechanics of hydraulic fracturing, J. Petrol. Tech., 9, 153-168.

Hudson, J.A., 1971, A critical examination of indirect tensile strength tests for brittle rocks, PhD thesis, University of Minnesota.

Maldonado, F., and S. L. Koether, 1983, Stratigraphy, structure, and some petrographic features of Tertiary rocks at the USW G-2 drill hole, Yucca Mountain, Nye County, Nevada, U.S.G.S. Open-File Report 83-732.

Scott, R. B., and R. W. Spengler, 1982, Structural framework of a potential nuclear waste repository, Yucca Mountain, Nevada Test Site, EOS Trans. AGU, 63, 1099.

Snyder, D. B., and W. J. Carr, 1982, Preliminary results of gravity investigations at Yucca Mountain and vicinity, southern Nye County, Nevada, USGS Open-File Report #81-1338.

Zemanek, J., E. E. Glenn, L. J. Norton, and R. L. Caldwell, 1970, Formation evaluation by inspection with the borehole televiewer, Geophysics 35(2), 254-269.

Zoback, M. D., J. Healy, J. C. Roller, G. S. Gohn, and B. B. Higgins, 1978, Normal faulting and in situ stress in the South Carolina coastal plain near Charleston, Geology, 6, 147-152.

Zoback, M. D., D. Moos, and R. N. Anderson, 1982, Determination of the horizontal principal stresses from wellbore breakouts, EOS Trans. AGU, 63, 1118.

APPENDIX: USW G-2 TELEVIEWER PHOTOS

TELEVIEWER LOG DATA SHEET

Well: USW G-2
Location: Nevada Test Site
Date logged: October 11, 1982 Tool No.: 1 Surface Panel: 1
Zero depth at: top of casing
Top of logged interval: 1730', top of water level in hole
Bottom of logged interval: 4110', hole blocked

Depth range (feet)	Tool settings Borehole gain	TV gain	Notes
1725 - 2395	8	184	
1918			Black band due to wireline jump
2118			Black band caused by resetting gate width
2395 - 2420	8	160	
2420 - 2475	8	162	
2475 - 2530	8	155	
2530 - 2615	7	155	
2615 - 2620	6	155	
2620 - 3065	7	155	
3065 - 3105	7	148	
3105 - 3125	6	148	
3125 - 3145	8	148	
3145 - 3285	8	138	
3285 - 4110	7	138	
3960			Borehole DC power adjusted
3935			"

Logged by: J. Svitek, S. Hickman

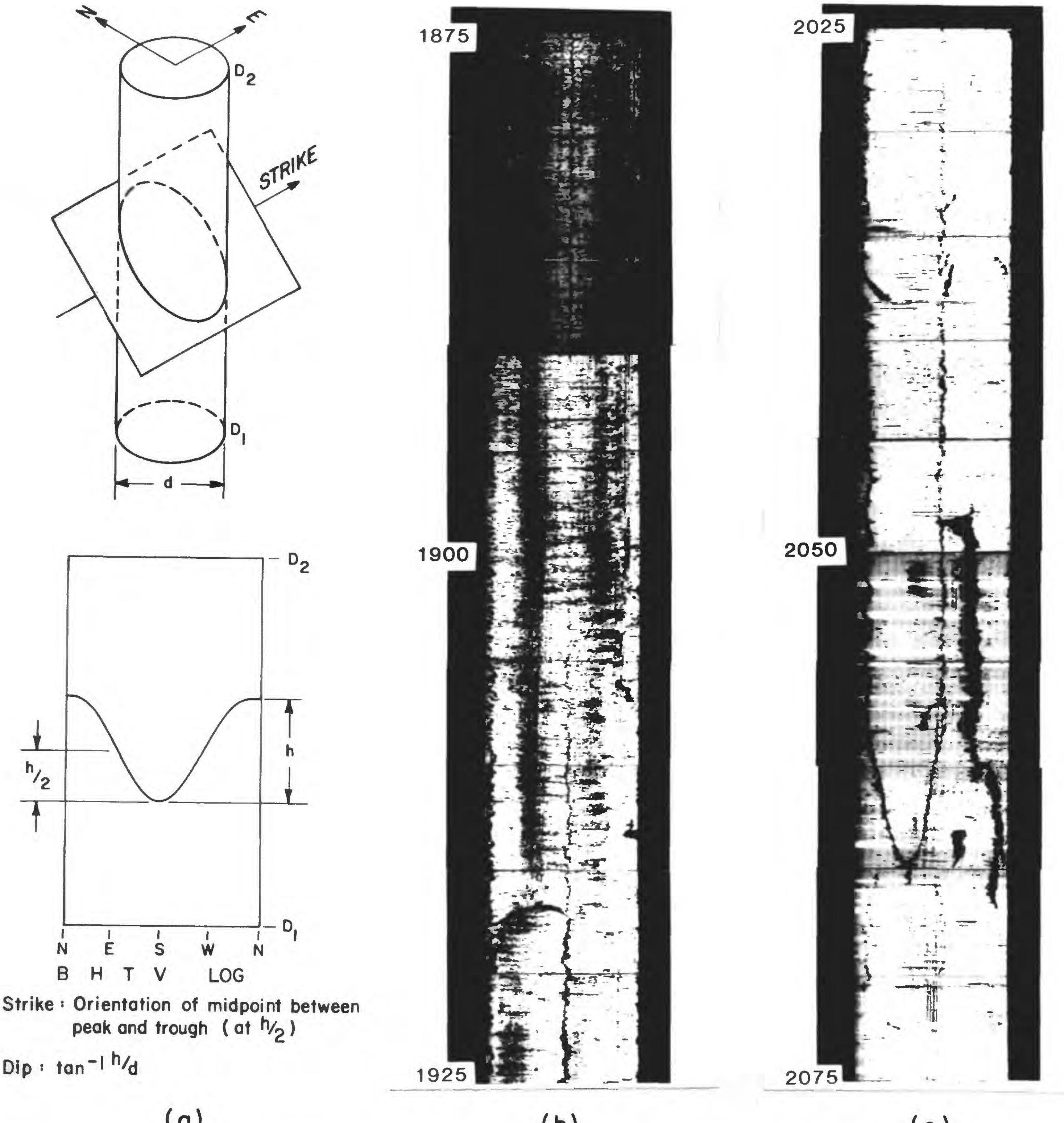

Figure 1. a) Isometric sketch of fracture or bedding plane intersecting borehole and corresponding borehole televiewer log [after Zemanek et al. (1969), fig. 7];
b) Televiewer picture from 571 to 587 m (1,875 to 1,925 ft), USW-G1 borehole, showing vertical drilling-induced fracture, borehole ellipticity, and sinusoidal trace of dipping fracture;
c) Televiewer picture from 617 to 632 m (2,025 to 2,075 ft) showing near vertical (+89° dip) fracture exiting borehole.

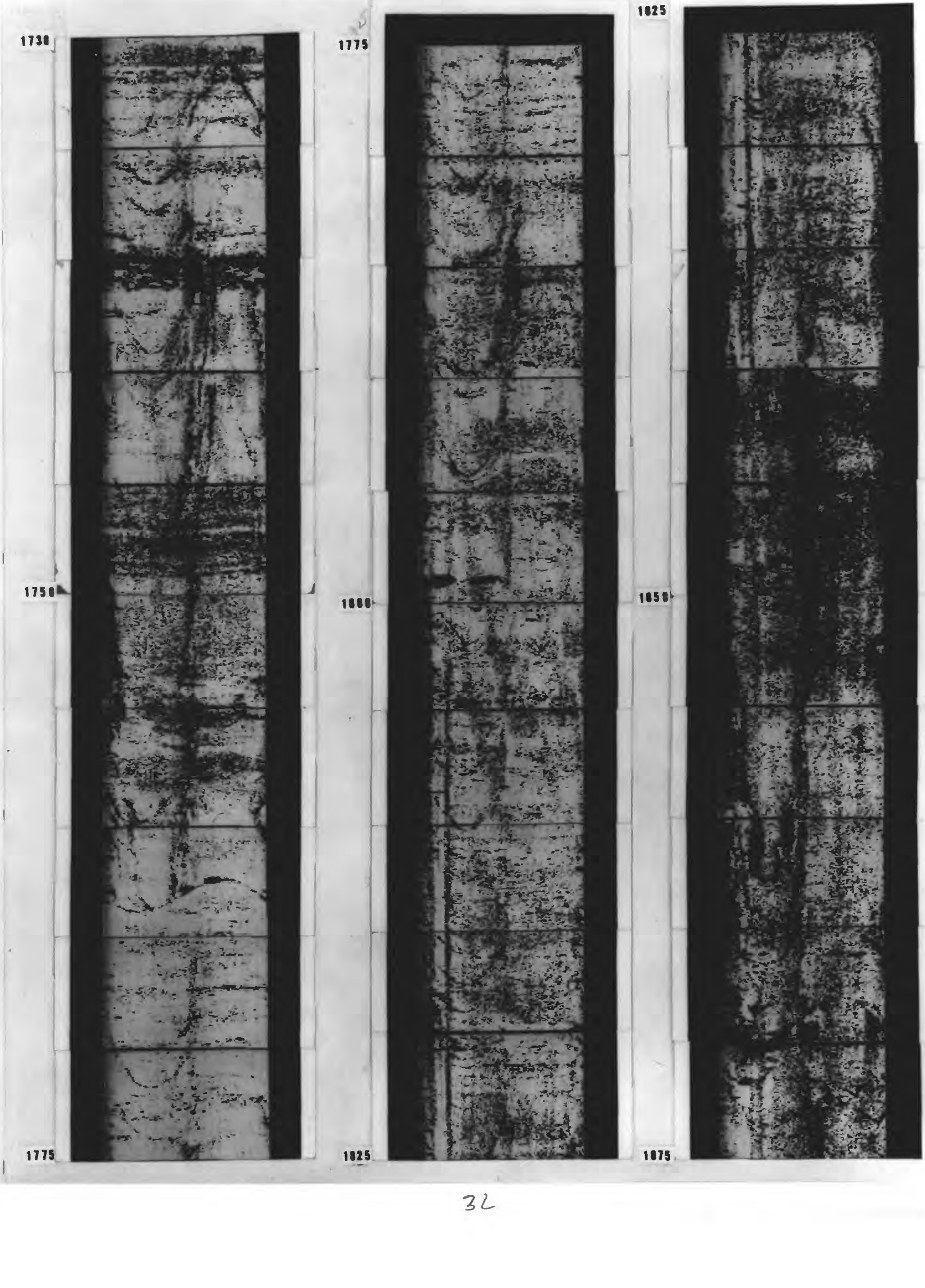

1730
1750
1775
1775
1800
1825
1825
1850
1875

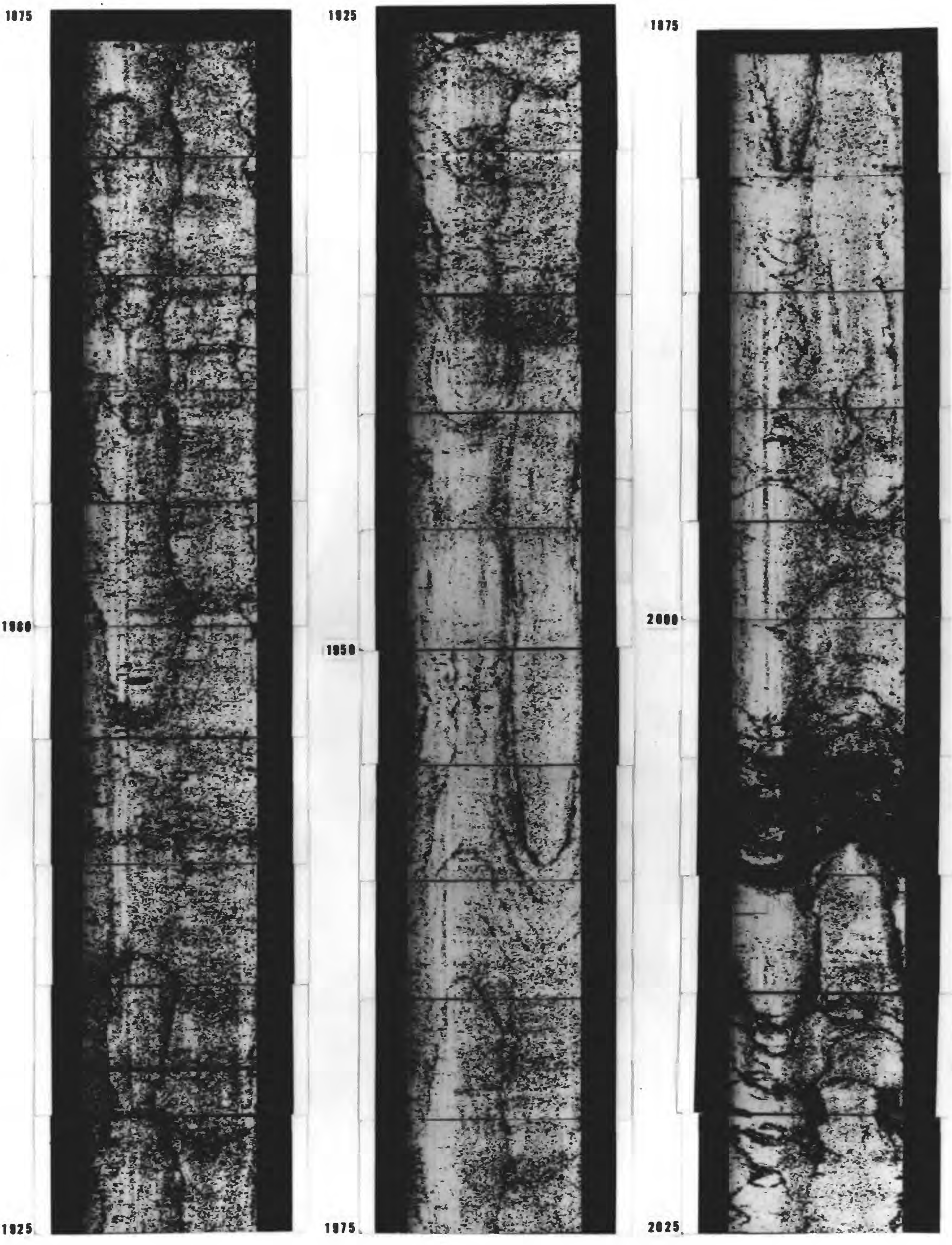
1875
1900
1925
1925
1950
1975
1875
2000
2025

2025

2050

2075

2075

2100

2125

2125

2150

2175

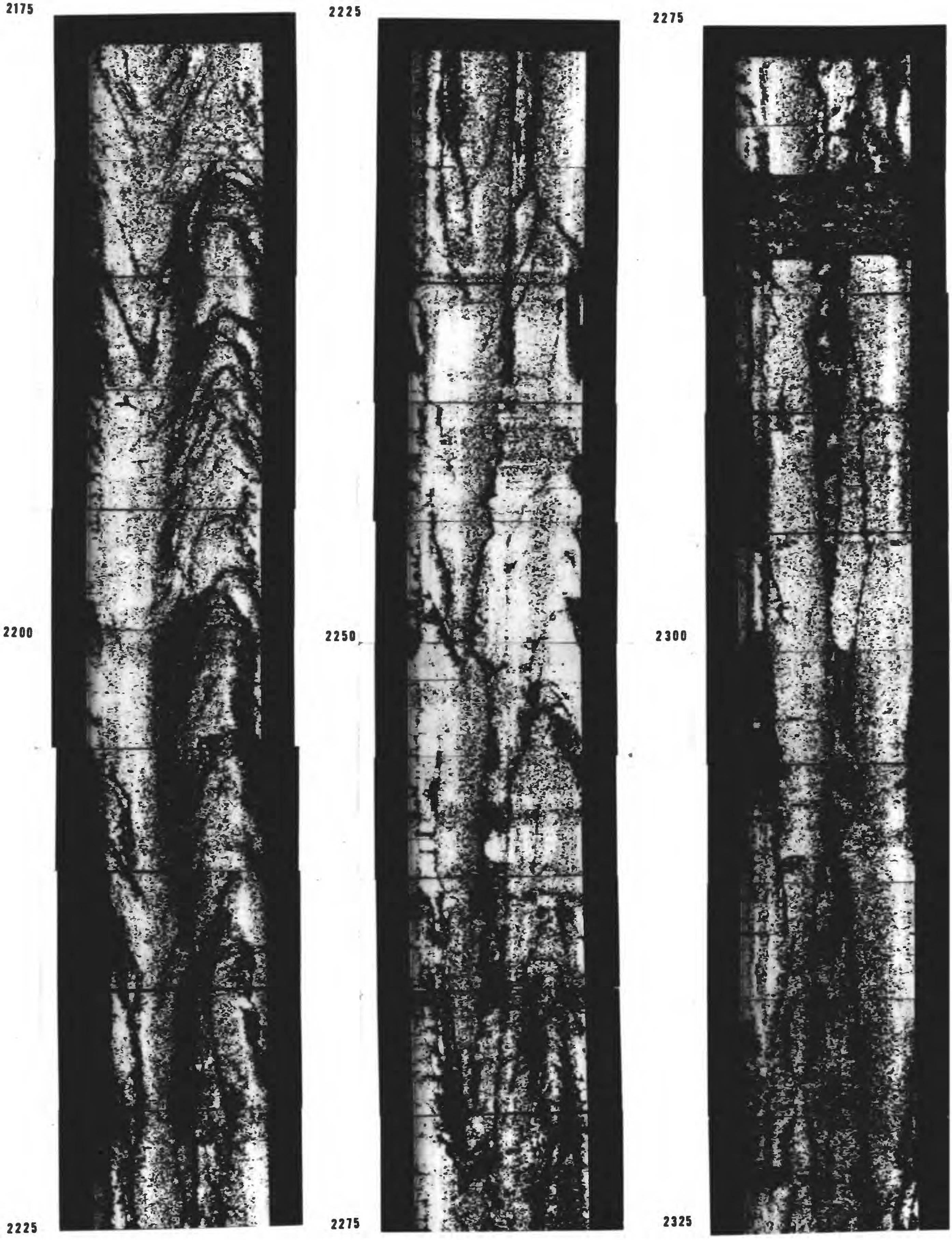
2175
2200
2225
2225
2250
2275
2275
2300
2325

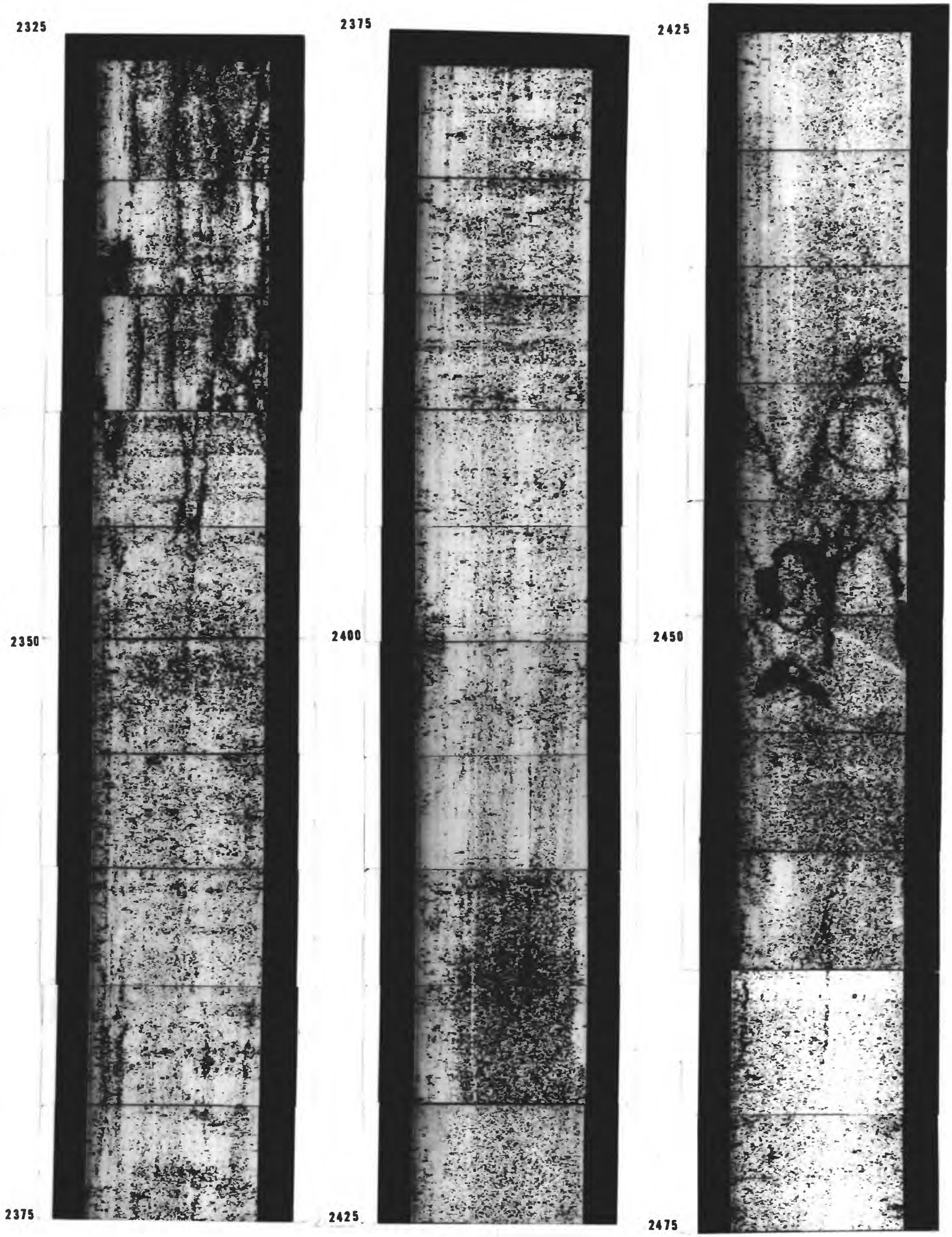
2325
2350
2375
2375
2400
2425
2425
2450
2475

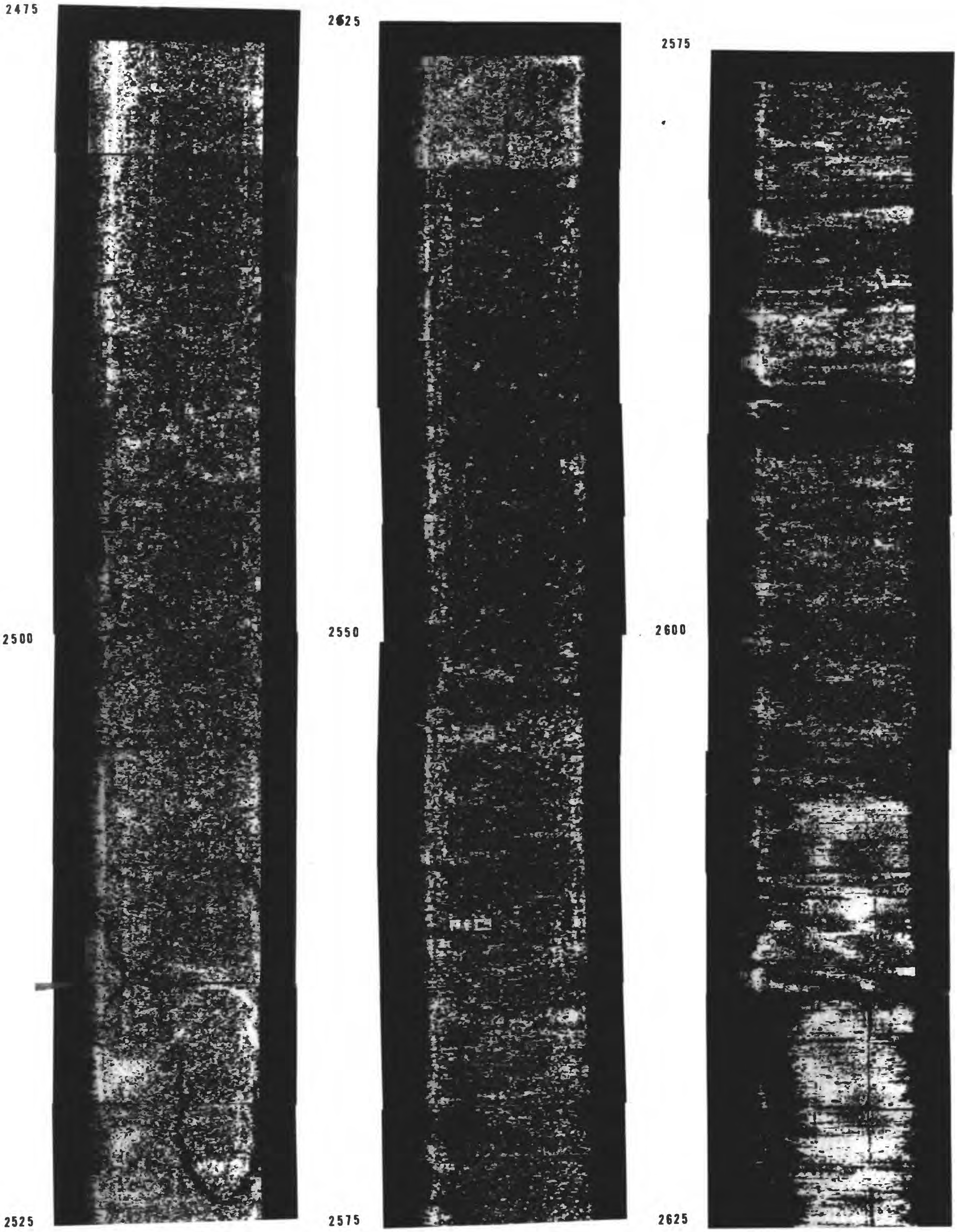
2475
2500
2525
2525
2550
2575
2575
2600
2625

2625

2650

2675

2675

2700

2725

2725

2750

2775

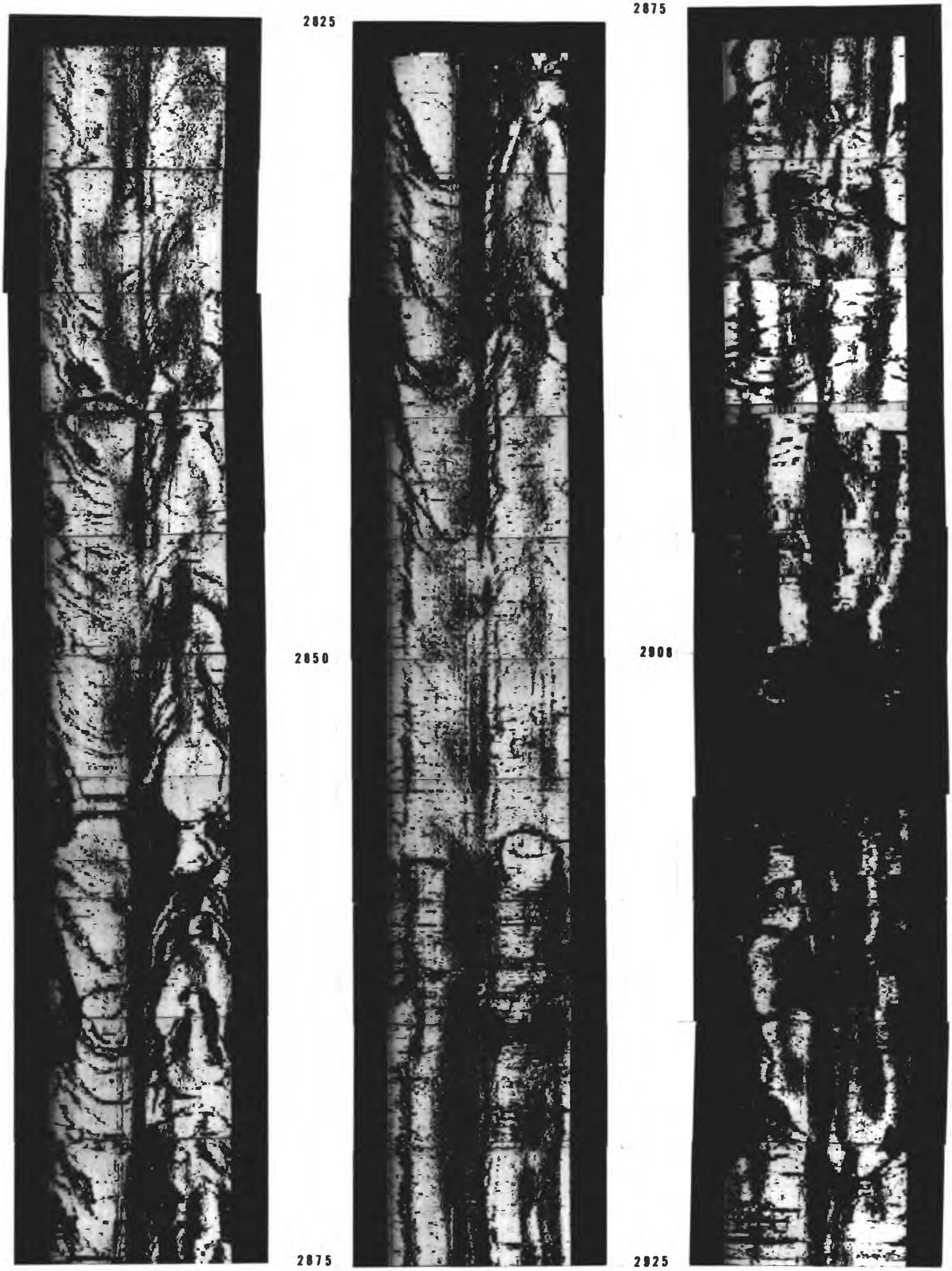
2775
2800
2825
2825
2850
2875
2875
2900
2925

2925

2950

2975

2975

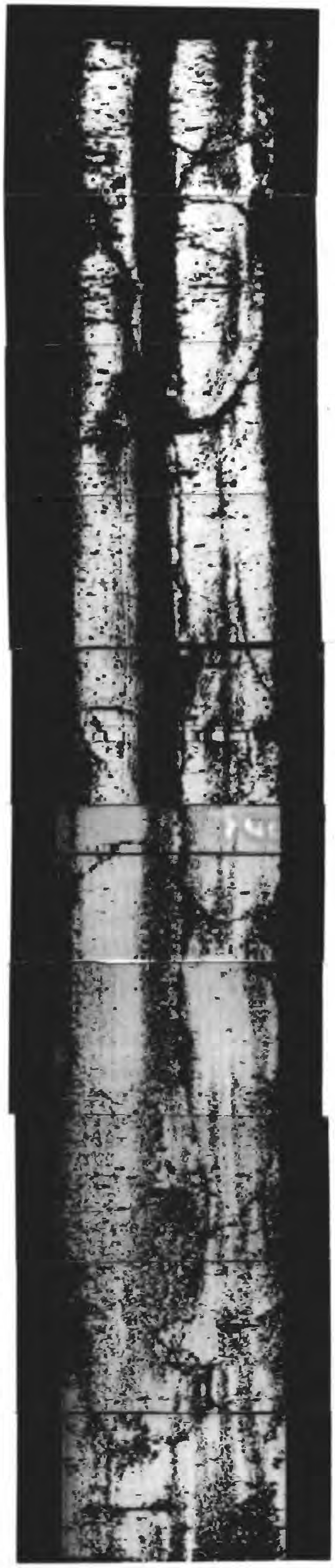

3000

3025

3025

3050

3075

3075

3100

3125

3125

3150

3175

3175

3200

3225

3225

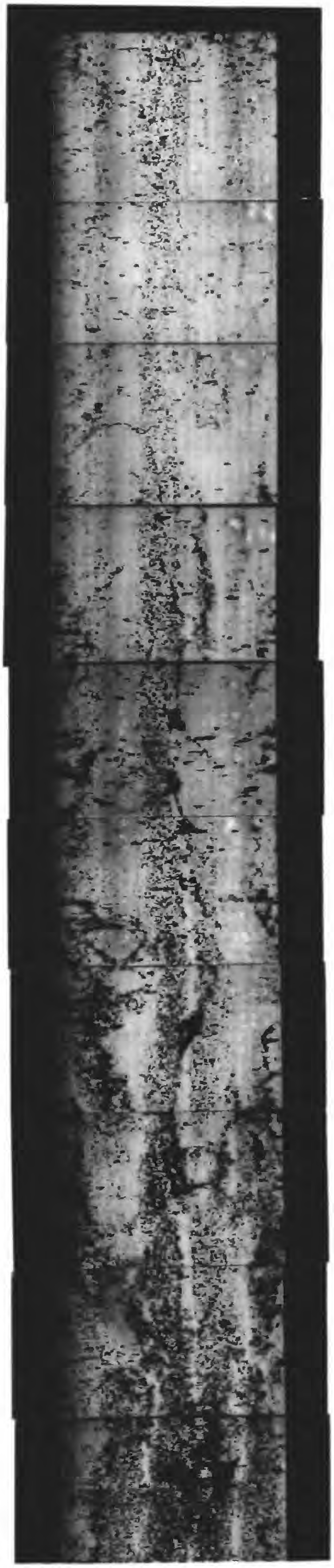

3250

3275

3275

3300

3325

3325

3350

3375

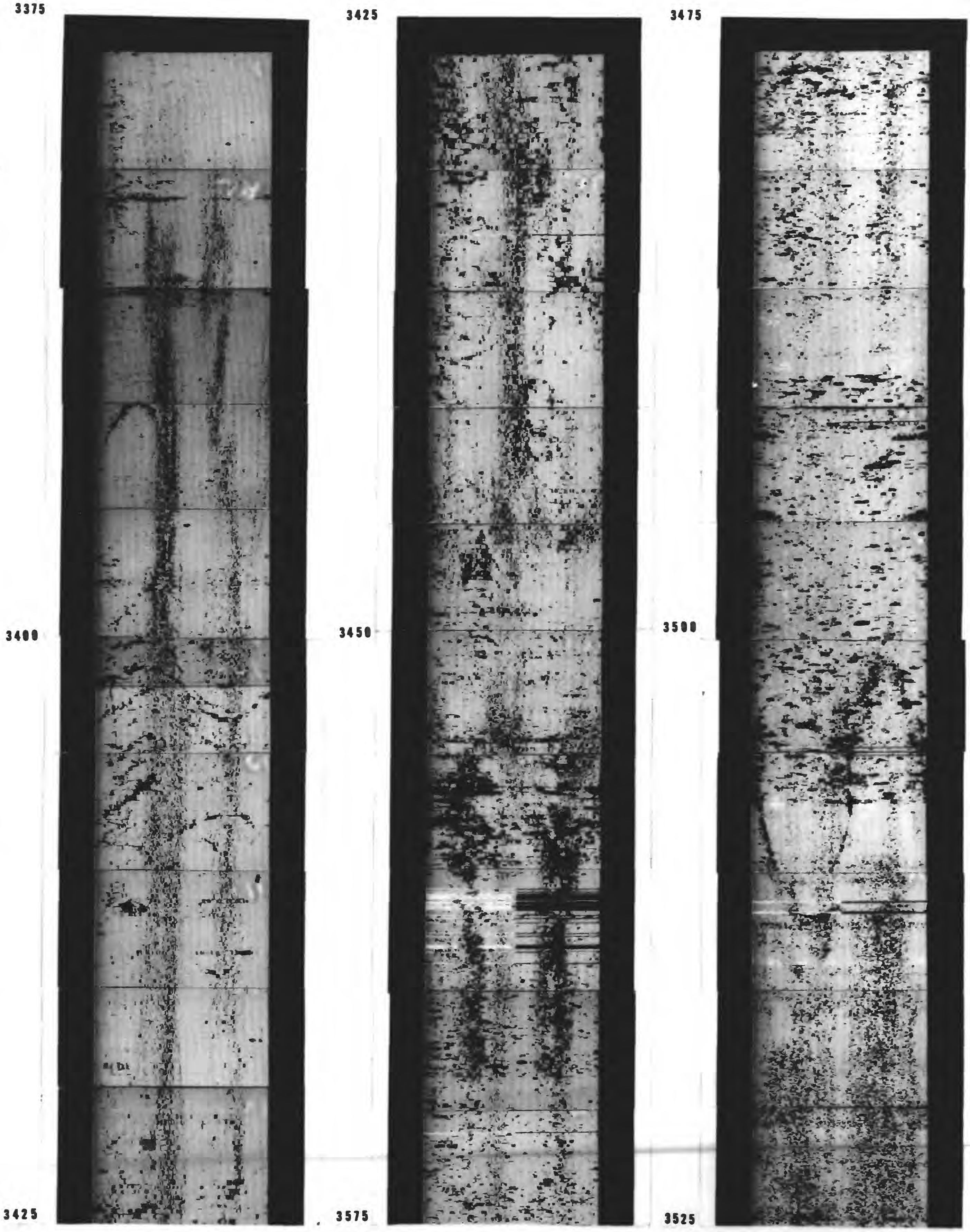
3375
3400
3425
3425
3450
3575
3475
3500
3525

3525

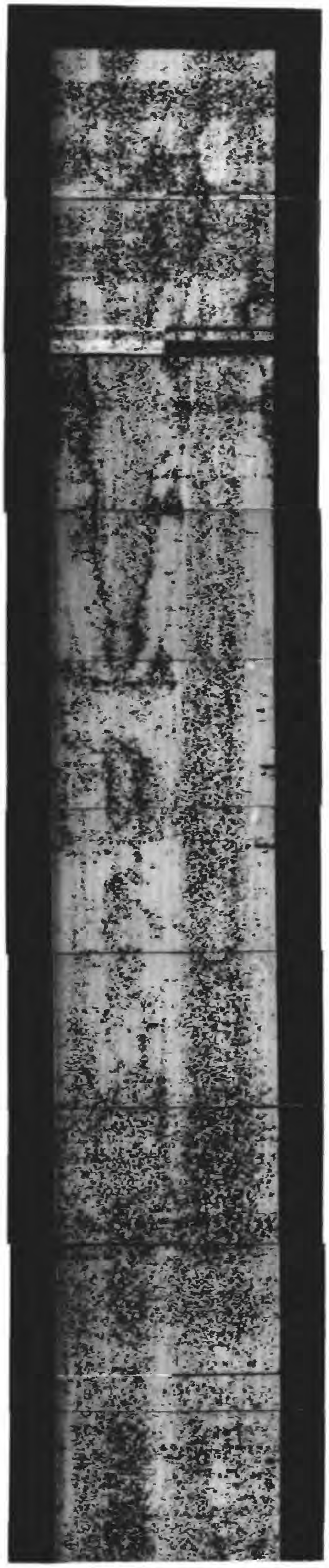

3550

3575

3575

3600

3625

3625

3650

3675

3675

3700

3725

3725

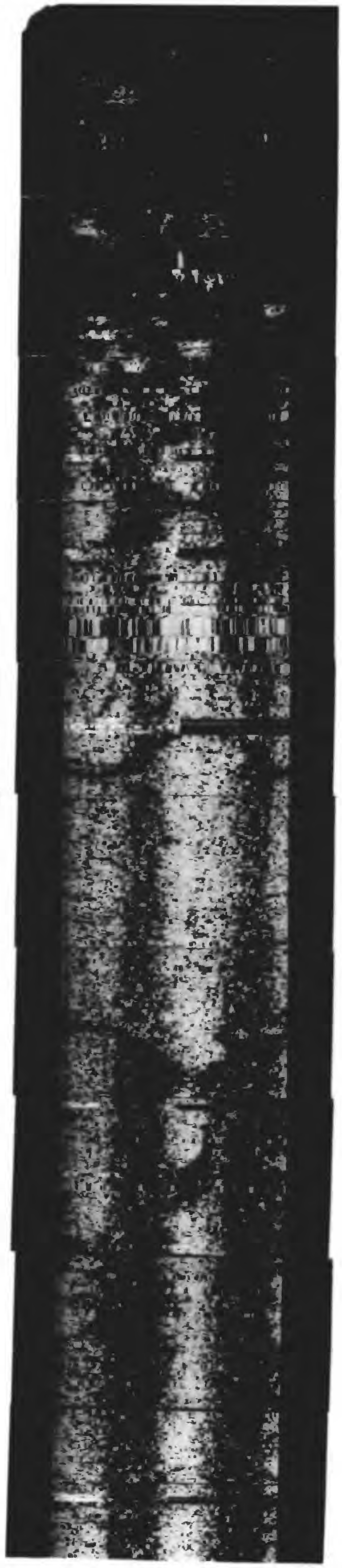

3750

3775

3775

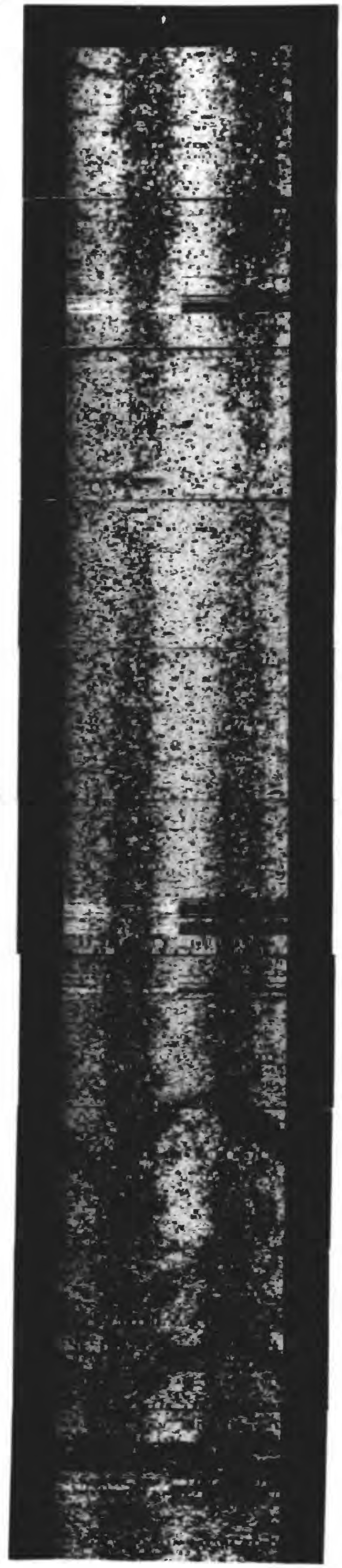

3000

3825

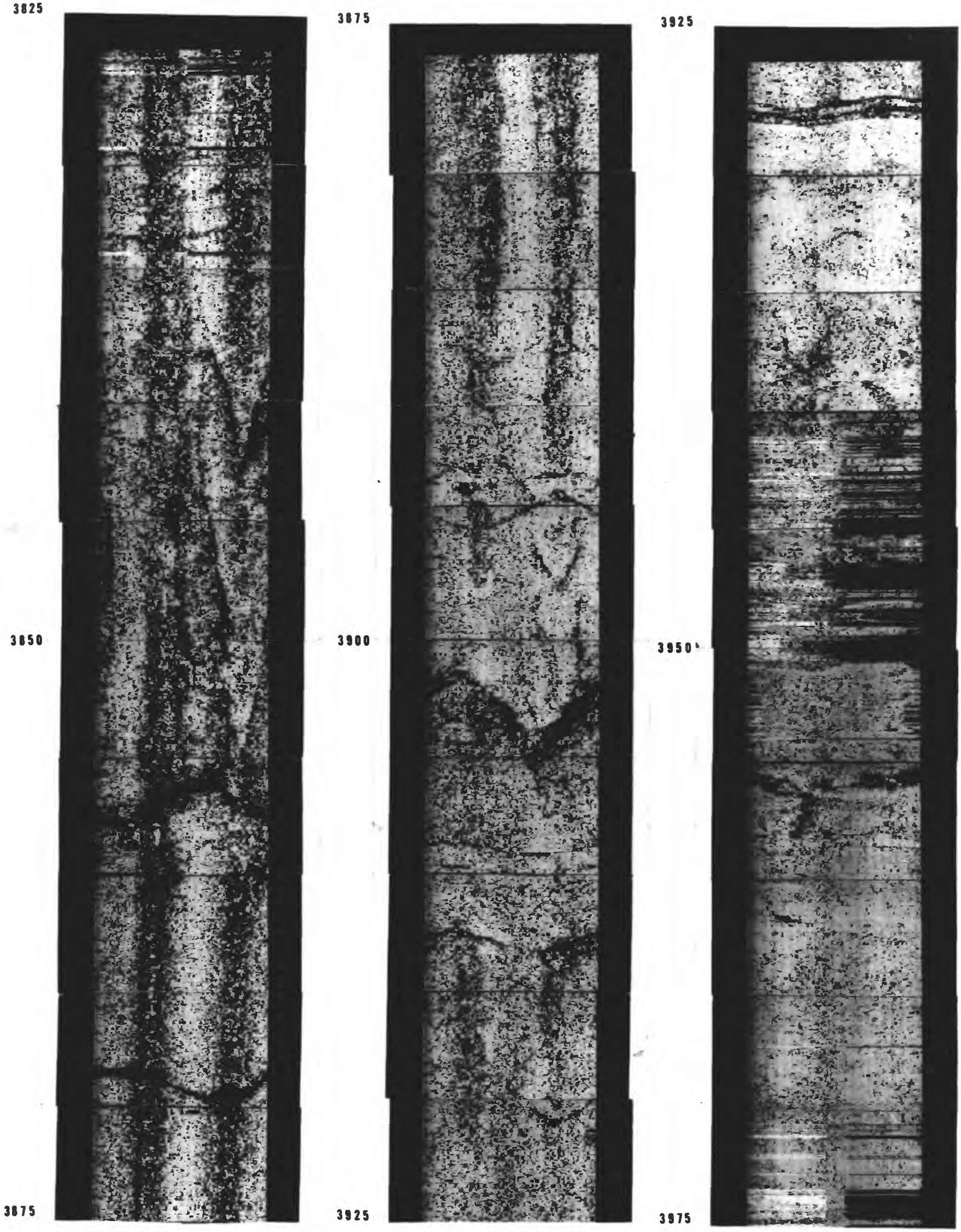
3825
3850
3875
3875
3900
3925
3925
3950
3975

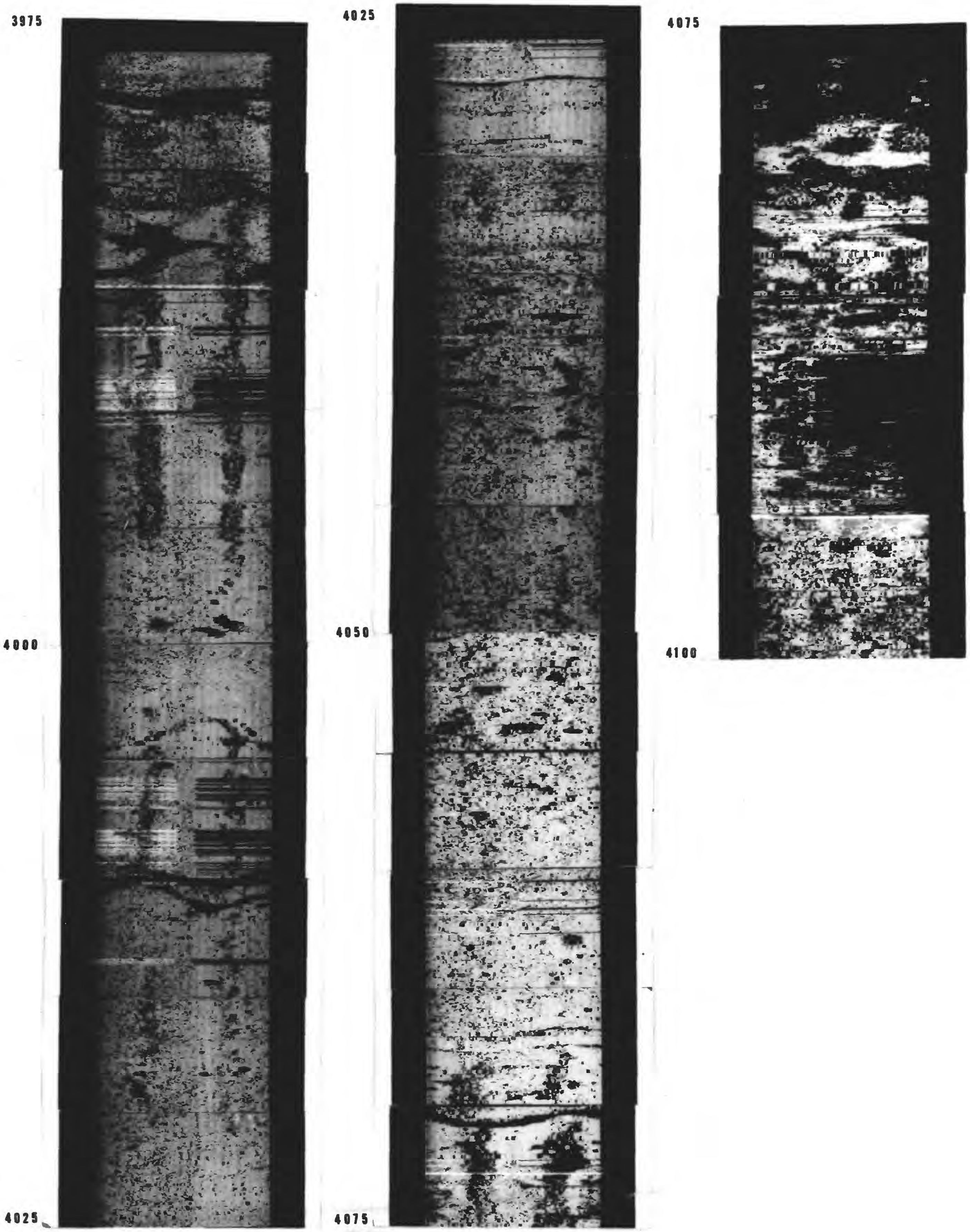
3975
4000
4025
4025
4050
4075
4075
4100